ATTENUATION CHARACTERISTICS OF STRONG SEISMIC GROUND MOTION IN INDIA

A Thesis Submitted
In Partial Fulfilment of the Requirements
for the Degree of
MASTER OF TECHNOLOGY

by

YEALURU J. J. PRASAD

to the

DEPARTMENT OF CIVIL ENGINEERING
INDIAN INSTITUTE OF TECHNOLOGY KANPUR

November, 1991

CERTIFICATE

It is certified that the work contained in the thesis entitled "ATTENUATION CHARACTERISTICS OF STRONG SEISMIC GROUND MOTION IN INDIA", by Sri Yealuru J. J. Prasad, has been carried out under my supervision and that this work has not been submitted elsewhere for a degree.

R P Singh
26.11.91

November, 1991

(Dr. Ramesh P. Singh)
Assistant Professor
Department of Civil Engineering
Indian Institute of Technology
Kanpur-208 016, India

ABSTRACT

Reliable assessment of seismic risk in a region requires knowledge and understanding of both seismicity and attenuation of strong seismic ground motion. In India strong ground motion records are almost non-existent. In recent years, some strong motion instruments have been deployed in the seismically active regions of the Himalaya. The high seismicity of the Himalayan region is attributed to the collision of Indian and Eurasian plates in the geological past. Presently, Indian plate is subducting beneath the Eurasian plate at a rate of 4-5 cm per year. Due to the motion of Indian plate, the collision boundary is seismically very active. The whole region has experienced many major earthquakes in this century. For the protection of life and property from earthquakes, it is essential to have an idea of seismic risk in the region. The seismic risk in a region can be assessed using attenuation of strong ground motion. In the absence of abundant strong ground motion data, empirical relations relating different measures of ground motion with earthquake parameters can be used to predict the level of ground motion in future earthquakes. The design of important structures such as nuclear power plants, dams and high-rise buildings uses estimates of ground motion. In the present work, we have made an effort to develop some attenuation relationships to calculate attenuation of strong ground motion in different Indian regions based on the past earthquake data. Attenuation relations have been developed for peak horizontal acceleration and peak velocity for different regions. We have also studied the intensity attenuation for different earthquakes of India, and similarity between the intensity attenuation and the ground motion attenuation is discussed. The ground motion relations for different regions of India have been compared with those of other geographical regions in the world. The attenuation relations derived in this work are proposed for use in a variety of Earthquake Engineering applications and in the preparation of seismic zoning map.

ACKNOWLEDGEMENTS

IT IS MY PLEASURE TO EXPRESS MY HEARTY GRATITUDE AND DEEP REGARD TO DR. RAMESH P. SINGH, MY THESIS SUPERVISOR, FOR HIS INVALUABLE GUIDANCE AND CONSTANT ENCOURAGEMENT THROUGHOUT THE PRESENT WORK.

I WISH TO EXPRESS MY DEEP SENSE OF GRATITUDE TO ALL THE FACULTY MEMBERS OF CIVIL ENGINEERING DEPARTMENT, IN PARTICULAR DRS. K. V. G. K. GOKHALE AND B. C. RAYMAHASHAY, FOR INTRODUCING ME TO VARIOUS COURSES.

I AM THANKFUL TO DRS. S. K. JAIN AND V. K. GUPTA FOR THEIR HELP DURING THE THESIS PERIOD.

PART OF THIS WORK HAS BEEN SUPPORTED BY DEPARTMENT OF SCIENCE AND TECHNOLOGY, NEW DELHI, UNDER HIMALAYAN SEISMICITY PROJECT. WE THANKFULLY ACKNOWLEDGE THEIR SUPPORT.

IT IS MY PLEASURE TO EXPRESS MY GRATITUDE TO ALL OF MY FRIENDS, IN PARTICULAR T. S. RAO, K. C. REDDY, VINOD AND VENKAT FOR THEIR HELP IN PREPARING THIS THESIS. THANKS ARE ALSO DUE TO SUNIL, SHAILESH, RAKESH AND SUMAN FOR MAKING MY STAY AT I. I. T. KANPUR, MEMORABLE.

FINALLY I AM EXTREMELY GRATEFUL TO MY PARENTS, SISTER AND BROTHER FOR THEIR CONSTANT INSPIRATION, BLESSINGS AND EXPEDIENT ADVICE IN THIS ENDEAVOUR.

NOVEMBER, 1991 (Y. J. J. PRASAD)

TO

AMMA AND NANNA GARU

LIST OF FIGURES

CHAPTER I

INTRODUCTION

1.1 GENERAL

The Himalayan belt is formed due to the collision of Indian and Eurasian plates in the past several million years. This belt is seismically active and earthquakes of varying magnitudes are being observed. Most of these earthquakes are associated with great loss of life and destruction of property. For understanding of the nature of earthquakes and for reliable assessment of seismic risk in the Himalayan belt, knowledge and understanding of seismicity and the attenuation of strong seismic ground motion are essential. One of the major problems in the Himalayan region is the frequent occurrences of earthquakes. Due to the vast natural resources in the Himalayan region, development of the region is being planned. For the utilization of its resources major projects such as Tehri dam have been proposed. People living in this region are concerned about their survival, due to the active seismicity of the region. In the light of the increasing seismicity, an appraisal of the relation of earthquake occurrences with geology and tectonics of the region is very essential to make an assessment of the seismic potentialities, for survival of the lives and natural resources, and in designing of the major structures. The designing of structures to resist earthquake ground motion is an important challenge to the Civil Engineers. This challenge can only be met if we develop ability to predict ground motion due to future earthquakes. Important structures such as nuclear power plants, dams, and high-rise buildings require

estimate of ground motion for earthquake resistant design. In the present work, we have made an effort to derive some empirical relations for different seismically active regions of India, which can be used to predict ground motion at the site of interest.

1.2 DIFFERENT MEASURES OF GROUND MOTION

Various parameters calculated from the strong earthquake ground motion records as shown in Figure 1.1, may be used for purposes of seismic design. Ground motion parameters such as peak acceleration, peak velocity and displacement are measured from ground motion record. Peak acceleration is most commonly used, other quantities used are peak velocity and response spectral values. The response spectrum is defined as the maximum response, to a given motion, of a set of single degree of freedom oscillators (for example mass-spring systems) having natural periods and damping. The response spectral values are useful in structural design because they take account of frequency of the structure. The response spectrum is maximum response to a given motion, of a particular structure.

Peak horizontal acceleration may be used in simplified procedures for evaluating liquefaction and in pseudostatic studies of slope stability. Peak acceleration has also been commonly used in the past as a scaling parameter to scale a normalized spectral shape and obtain response spectra for analysis of structural response.

1.3 MEASUREMENT OF STRONG GROUND MOTION

Special instruments are required to measure strong motion. Ground motion is recorded in two horizontal and one vertical

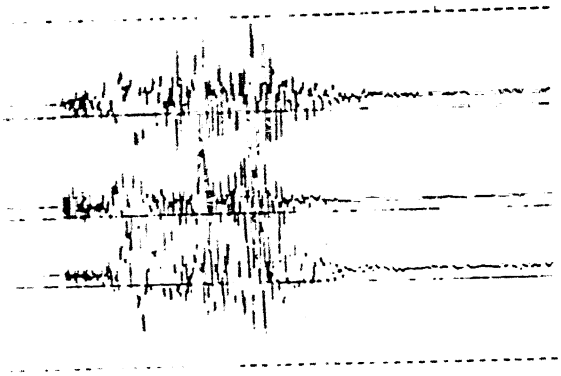

Fig. 1.1 A typical strong ground motion record

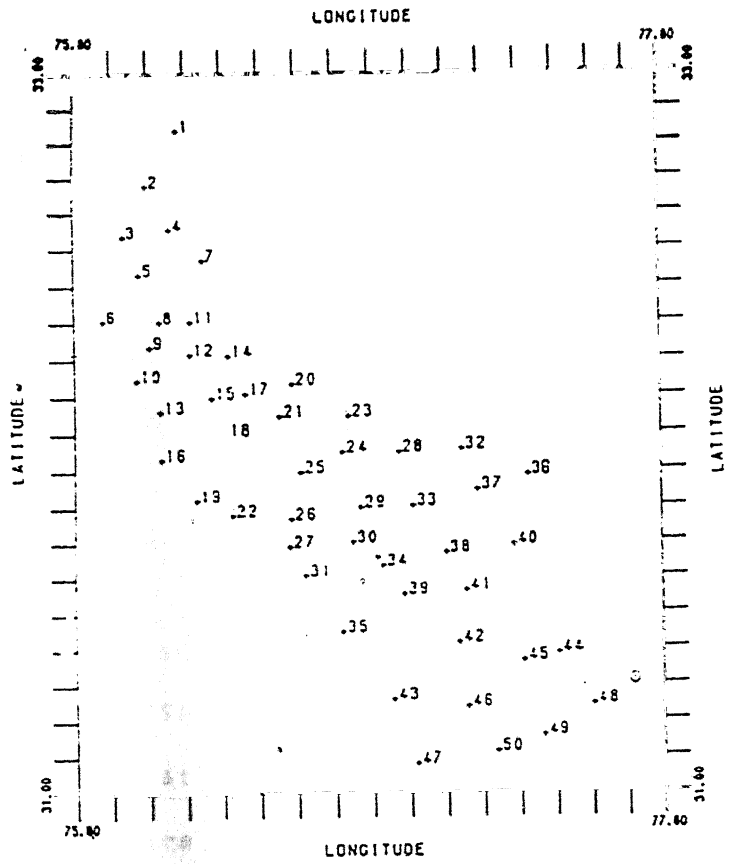

Fig. 1.2 Location of stations in Kangra strong motion arrav

direction on photographic film. The old instruments used photographic paper instead of film. The modern instruments make digital recording on magnetic-tape cassettes or in solid-state memory units. Strong motion instruments are turned on by the earthquake ground motion itself. They are unattended and are protected from weather and vandalism by a shelter. A typical example of the record obtained from accelerograph is shown in Figure 1.1.

The strong motion recording requires an extraordinary degree of patience and diligence. Instruments are deployed for decades to record strong motion of a major earthquake that is strong enough and near enough to make a record. A large number of instruments are required to get a strong motion record of an earthquake in a seismically active area. Special efforts are required to ensure that a high percentage of instruments is operational when an earthquake does occur.

1.3.1 STRONG-MOTION STUDIES IN INDIA

In India strong motion recording was almost non-existent. The first strong motion record is available from Koyana earthquake which triggered in 1967. Strong motion in the Himalayan region was first recorded in 1986. Micro-seismic activities due to Reservoir Induced Seismicity at various dam sites are being monitored for the last twenty years, but the recorded strong motion is very less. The Department of Science and Technology, Ministry of Science and Technology under national strong motion network program, has installed many strong motion accelerogaphs in the seismically active regions such as Assam and Shillong.

Data obtained from such strong motion accelerographs are very

valuable. These data provide information to evaluate the nature of the source mechanism, the influence of the wave propagation path, tectonic features of the region, and are useful in the structural engineering design.

Presently two strong motion arrays are in operation, which cover a large region. These arrays are:

(1) Kangra Array covers Kangra region of Himachal Pradesh (Figure 1.2) and

(2) Shillong Array covers Shillong region of the states of Meghalaya and Assam (Figure 1.3).

1.4 OBJECTIVES OF THE STUDY

The evaluation of design parameters in India has been mainly based on data obtained in western U.S.A.. For proper design parameters, the knowledge of strong ground motion data is required. We have made an effort to use strong motion data from the recent strong motion arrays and have developed attenuation relations for different regions of India.

The estimation of ground motion at any location, is based on the analysis of strong motion records available from nearby regions. The strong ground motion data for India is very limited. Due to various limitations it is not possible to employ strong motion instrumentation close enough to get an idea about the strong motion in the close vicinity of site of interest. Therefore, in the present study, we have made an effort to develop some empirical relations between different measures of strong ground motion and the earthquake parameters. The present work has been carried out with the following objectives:

(i) to study the attenuation of peak horizontal acceleration

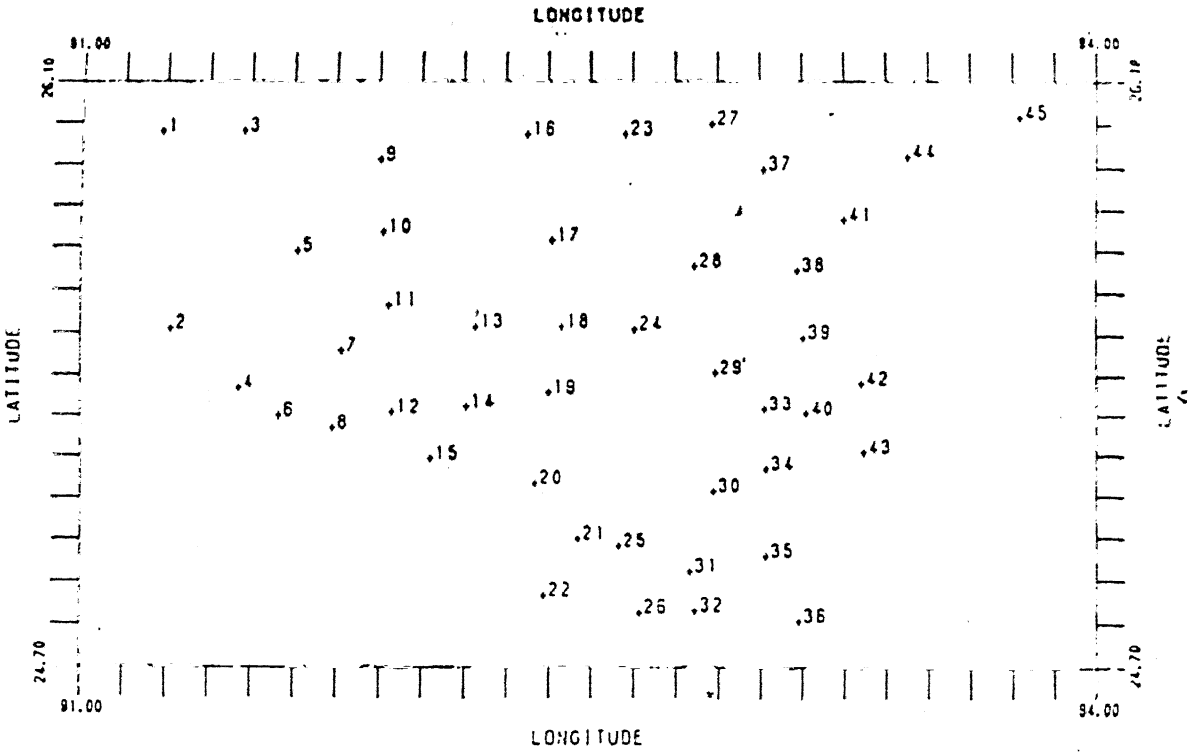

Fig. 1.3 Location of stations in Shillong strong motion array

with distance, in different regions of India,

(ii) to study the attenuation of peak horizontal velocity with distance in different regions,

(iii) to obtain the acceleration-intensity correlation for northern India using the four variable covariance,

(iv) to compare the acceleration-intensity correlation of India with that of various geographical regions using the four variable covariance,

(v) to compare the acceleration-distance dependence of different countries/regions with that of India, and

(vi) to study the attenuation of earthquake intensity with epicentral distance for different Indian earthquakes.

1.5 ORGANISATION OF THE THESIS

Besides this introductory chapter, the thesis contains four more chapters to cover the present work. Chapter II gives a brief summary of Seismicity and Seismic zoning of India. We have discussed the seismicity of different regions and its relation with tectonic features. The high seismicity of the Himalayan region and the present geodynamic process in the region has also been discussed. Chapter III gives different attenuation models of strong seismic ground motion. The attenuation relations developed for various parts of the world have also been discussed. In Chapter IV, some of the correlations for strong seismic ground motion for India have been derived. Conclusions and Recommendations for further work have been given in Chapter V.

CHAPTER II

SEISMICITY OF INDIA

2.1 INTRODUCTION

Indian land mass is geologically divided into three major units: Himalaya, Indo-Gangetic plains and Peninsular shield. Each geological unit is characterised by different seismicity. Himalayan frontal arc, flanked by the Chaman Fault in the west and Arakanyoma in the east, is seismically one of the most active regions in the entire Alpide belt. The northern boundary of the Indian plate is defined by the belt of earthquakes through Sulaiman and Kirthar shear zones in the west, the Himalaya in the north and the Burmese arc in the east. Recent studies of focal mechanism solutions for earthquakes occurring in the Himalayas and nearby regions have shown left-lateral motion along the southern portion of the Sulaiman Range, right-lateral along the Himalayan flank of the Assam syntaxis, and right-lateral along Naga hill flank (Singh and Gupta 1980). These mechanism solutions are consistent with the under thrusting of the Eurasian plate by the Indian plate. In accordance with the plate tectonics hypothesis, the current tectonic activity in Asia is considered to be a consequence of progressive continental collision between India and Eurasia (Dewey and Bird 1970). Continental reconstructions shows that India and Eurasia have been converging steadily at the rate of 10 to 15 cm/year since Cretaceous. However, since collision in Eocene, the rate decreased by one half (Molnar and Tapponnier 1975). For a better understanding of seismicity and tectonics at continent-continent collision boundary, it is necessary to have a good knowledge of the crustal and upper mantle structure beneath

the Himalaya and Tibet plateau region.

Holmes (1966) has given a crustal section extending from the Arabian sea up to the Verkhoyansk mountains. He believes that the large thickness of 60 km beneath the Himalayas and Tibetan plateau, which is almost double that of normal thickness of continental crust has been brought almost by an under-thrusting of the crust of Indian shield beneath the Himalayan ranges and Tibetan plateau and beyond. The origin of Indo-Gangetic trough is also attributed to the downward dipping of the Indian shield during its northward drift (Holmes 1966). Crustal thickness beneath the Gangetic basin has been reported to be 40 km by Choudhury (1975) from surface wave studies.

2.2 SEISMICITY OF HIMALAYAN REGION

One of the major problems in the Himalayan region is the frequent occurrences of earthquakes. As these regions are undergoing rapid developments and many projects such as Tehri dam are being planned, an appraisal of the relation of the earthquake occurrences with the geology and tectonics of the region is very essential to assess seismicity of the region. About two-thirds of India is earthquake prone area where earthquakes are frequently occurring. The states of Kashmir, Panjab, Himachal Pradesh, Uttar Pradesh, and Bihar, the Bihar-Nepal boarder, Kutch in Gujarat and the Andaman islands belong to earthquake prone region. These regions are close to the collision boundary of different plates and is attributed to the geodynamic process.

The moderate Garhwal earthquake of October 20, 1991, is part of the ongoing geodynamic process that has formed Himalayas over the past 40 million years. The earthquake is the result of sudden

release of compression strain energy which over decades had been slowly accumulated in the rocks of the region. As they reached their breaking point, these rock masses snapped or slipped along some weak zones or an earlier scar. The compression in this case is due to the continued northward motion of Indian plate pushing against already buckled and thickened Tibetan plateau, as it is dragged at its base by a gigantic convection current rising from deep below the crust. As the rocks are strong and even their fractured surfaces tend to offer resistance to motion due to friction, the continued compression does not result into a steady uniform motion. Instead, it manifests itself in a cycle of sticking and slipping, slowly shrinking for a while and then stopping as the resulting strain exceeds its strength. Likewise the continuing northward convergence of India towards Tibet takes place in spurts, as accumulating strains reach the minimum strength of rocks. A major earthquake releases most of the accumulated strain, and the Himalayan range lurches forward by a few metres in a sudden leap. Those parts of the Himalayan boundary (Figure 2.1) which have not ruptured in the last 300-600 years can have a current strain of around 8 metres. A slip of this order would, in turn, result in an earthquake of magnitude greater than 8 or so. Such potentially dangerous regions of an active boundary are called seismic gaps. The Garhwal earthquake of October 20, 1991 occurred in the central Himalayan seismic gap lying between the rupture zones of the Great Kangra (1905) and Bihar-Nepal (1934) earthquakes.

Kumaun Himalaya is a part of the Himalaya in which earthquakes occur very frequently. The epicentres of different earthquakes are shown in Figure 2.2. The distribution of

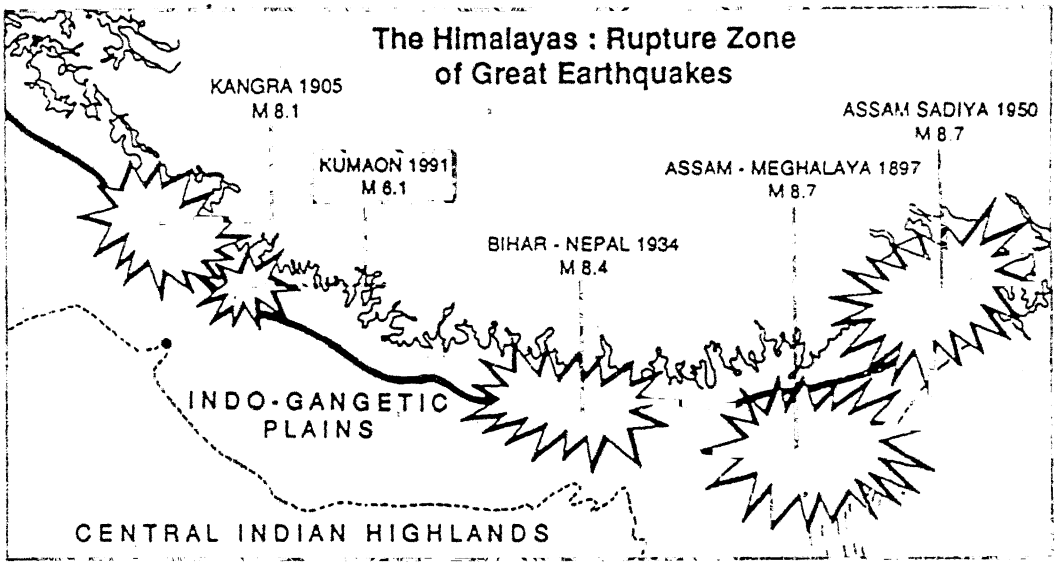

Fig. 2.1 Epicentres of great Himalayan earthquakes

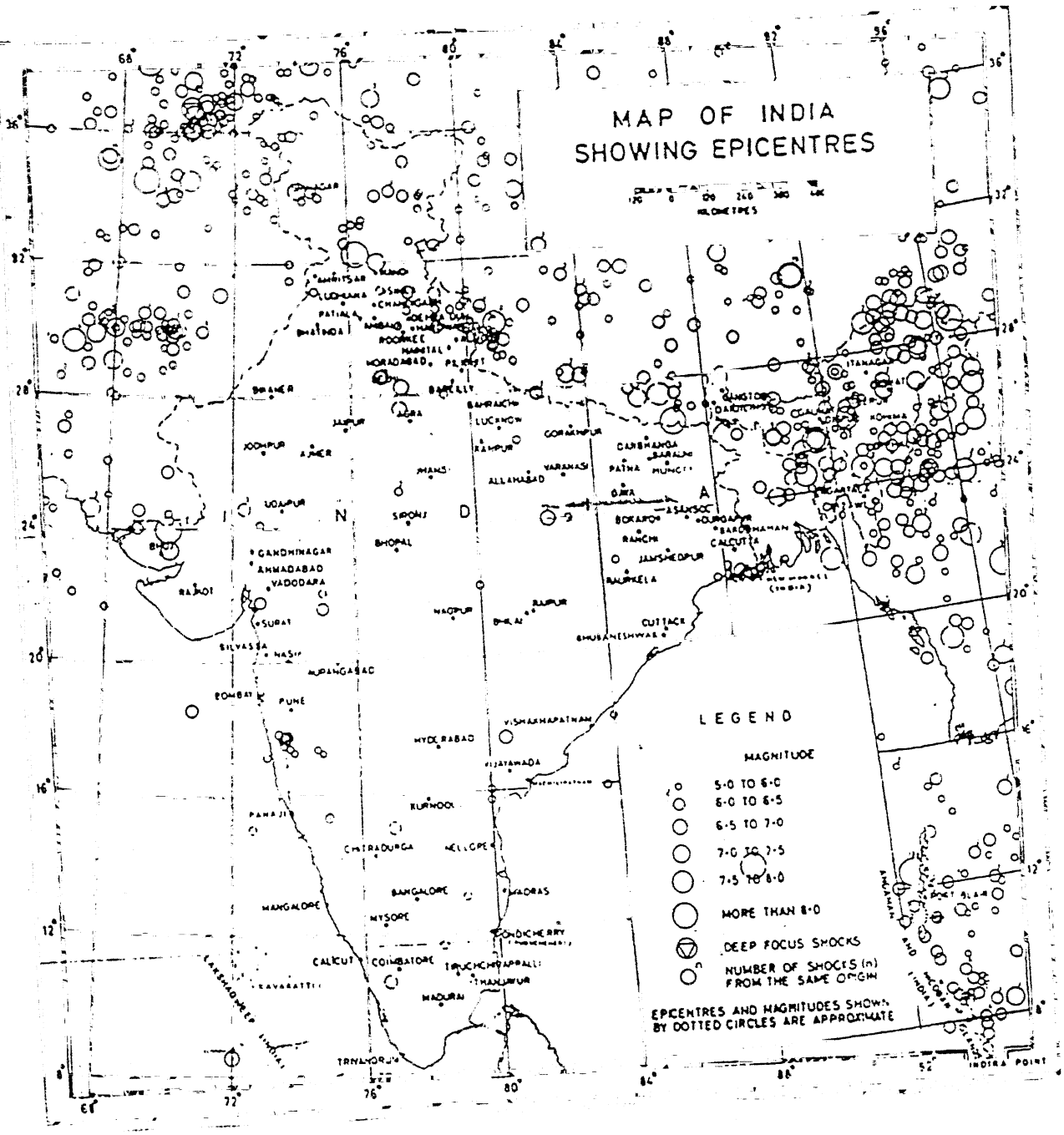

Fig. 2.2 Epicentres of Kumaun Himalayan earthquakes

epicentres shows general scatter, and definite associations with known thrusts and faults are not known. However, the epicentres are mostly confined to the nappe zone (Valdiya 1964), though epicentres are also noted in the Tethyan belt in the north and Siwalik belt to the south of this zone. Systematic records of earthquake occurrences in the Himalaya are available only of the recent times. This is mainly due to lack of a network of seismological stations in the region, and even now most of the areas are not fully covered by such network. Therefore, only very scanty information about the exact location of earthquake epicentres in the Himalaya is available. It happens that location of the most of the epicentres have been determined by using teleseismic data recorded in other parts of the country. The data for local and minor earthquakes are not available for most of the areas and thus, it is very difficult to pin-point the association of epicentres of shallow earthquakes, which are mostly responsible for damage at or near the ground surface, are of common occurrence in the Himalaya and these represent the manifestations of the tectonic processes in action in crust and upper mantle in the region.

2.2.1 THE SIWALIK BELT

The Siwalik belt in Bengal, Bihar, Uttar Pradesh and Himachal Pradesh in general has shown earthquakes of higher magnitude indicating presence of large compressive forces which lead to greater strain build-up. These enhanced compressive forces could be visualized if the presence of converging sub-crustal currents along such a zone is assumed. Siwalik belt in Himalaya, during the last hundred years has shown evidences mostly of minor

earthquakes, but possibilities of a major earthquake as observed in Bihar and other places can not be ruled out.

2.2.2 SEISMO-TECTONIC FEATURES OF KANGRA REGION

The tectonic environment of Himalayas is shaped during early Tertiary times due to the mountain building process. Among the various tectonic features, two are of prominence which can be traced all along the length of the Himalayas. These features are essentially thrust sheets. The tectonic feature separating Tertiary from mesozoic is the Main Boundary Fault (MBF) and Mesozoic from central crystallines is the Main Central Thrust (MCT). Apart from two regional tectonic features of prominence, there are local thrust sheets and tear faulting which demonstrate the neo-tectonic activity of the Himalayan region.

The MBF and other thrust sheets are considered as the potential tectonic sources for earthquake activity in the region. It is believed that the movements along Satilta thrust in the Beas river section may have been responsible for the great Kangra earthquake of 1905. Figure 2.3 shows the tectonic features and earthquake epicentres of magnitude greater than 4.0. The tectonic features and seismic activity clearly indicate a northwest-southeast trend.

2.2.3 SEISMO-TECTONIC FEATURES OF SHILLONG REGION

Shillong region in India has been identified as one of the six most potential sites of the world. Geologically, this region can be broadly classified into four geotectonic units, namely, Arunachal Himalayas, Lohit Himalayas, Patkoi-Naga-Lushai-Arakan Yoma (Indo - Burma) hill ranges and Shillong plateau-Assam basin.

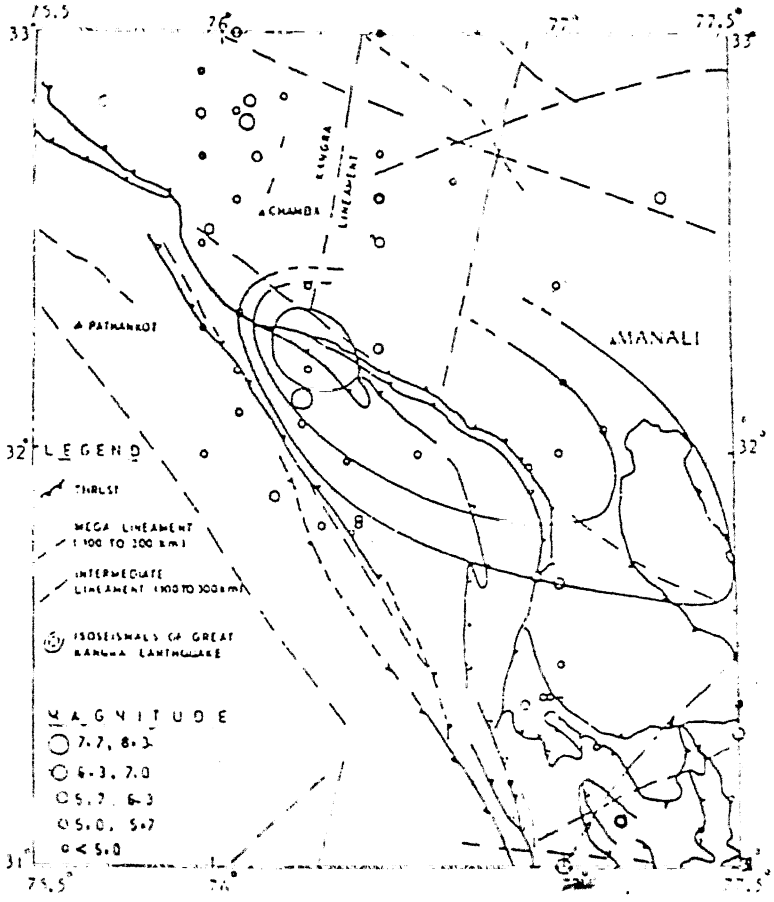

Fig. 2.3 Tectonic features and epicentres of different earthquakes in the Kangra region in Himachal Pradesh

Shillong massif forms the basement on which the alluvium and unfolded Tertiary formations of Assam basin has been deposited. The contact of the surrounding geotectonic units with the Shillong plateau is marked by conspicuous thrust and tear faults. Two prominent tectonic features forming the boundary of Shillong plateau towards west and south are the Dhubri and Dauki tear faults, respectively.

The plateau is bounded by Main Boundary Fault in the north west, towards northeast by Mishmi and Lohit thrusts, towards southeast by Naga thrust belts and on the south by Dauki tear fault which merges towards east with Haflong-Disang thrust zone. This complex tectonic regime surrounding Shillong plateau reveal that the area has experienced great compressive stresses and resulting distortions due to northward and eastward movement of the Indian plate. Apart from the complex tectonic features, Shillong has experienced number of earthquakes. This indicates that the Shillong plate and its adjoining regions have high seismic status. The seismic activity along the Dauki-Haflong fault zone is comparatively lower and a seismic gap has been postulated along this fault zone. Figure 2.4 shows the tectonic features and epicentres of past earthquakes in the region.

2.3 SEISMICITY OF INDO-GANGETIC BASIN

An analysis of the earthquakes that occurred in the present century indicates that the majority of them occured either in the Indo-Gangetic basin or in the Himalayan belt, especially along the southern margin of the mountain arc. The most important geological event, subsequent to the upper Siwalik and the glacial epoch, was the filling up, by sub-aerial and fluviatile deposits, of the

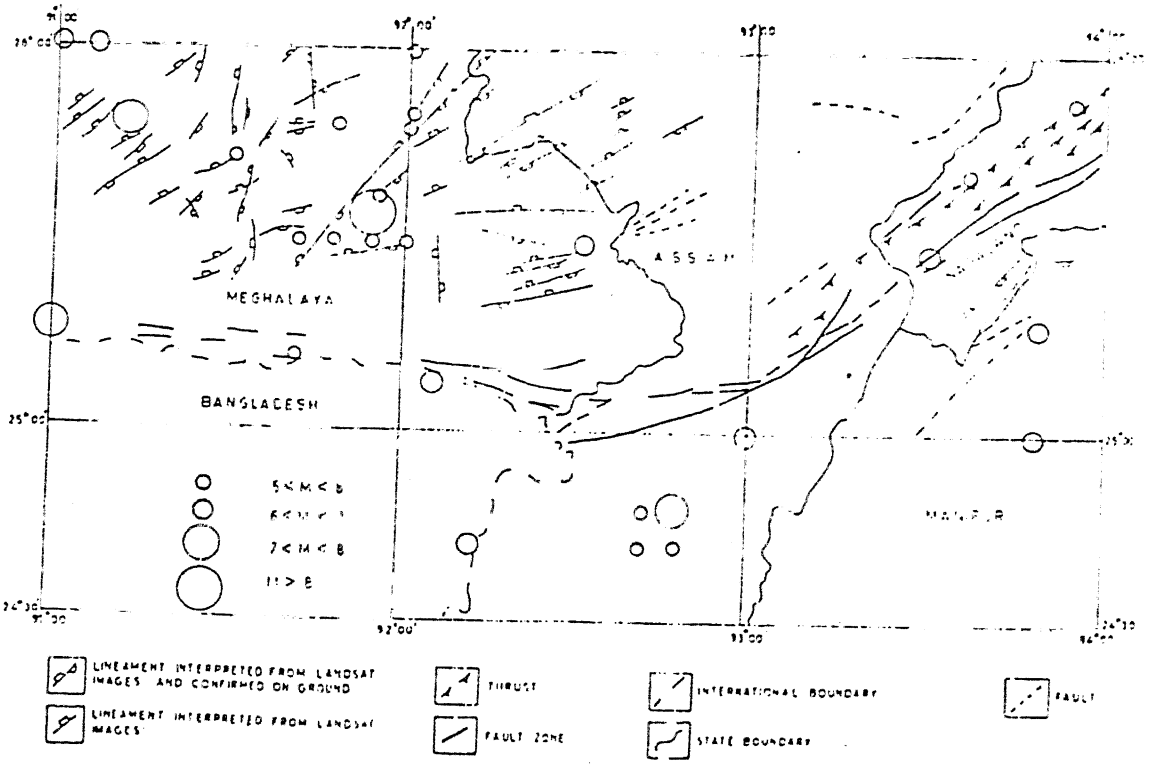

Fig. 2.4 Tectonic features and epicentres of different earthquakes in Shillong region

Indo-Gangetic trough, the great downwarp lying between the northern edge of the peninsula and the recently built Himalayan chain. The Gagetic basin is 250 miles wide in its broadest part and 1500 miles long from Sind to the outskirts of the Arakan Yoma (Figure 2.5).

In the Indo-Gangetic basin three significant linear clusters of epicentres (Figure 2.6) are noticed. These are,

(i) The Hindukush region in the north-west extremity,

(ii) The Kuman-Nepal boarder in the middle and

(iii) North-eastern Assam and adjoining regions (Valdiya 1976).

It is noticed from Figure 2.6 that the seismicity of the Kumaun-Nepal boarder area is related to the Muradabad fault. The unmistakably linear spatial distribution in the north-south direction of the epicentres the Dharchula area (Valdiya 1976) is suggestive of tear movement, although there might have been concomitant dip-slip movement along the thrusts. Interestingly, Ichikawa et al. (1972) found strike-slip faulting to be predominant in central Himalaya. The focal mechanism (Fitch 1970) suggests strike-slip movement in a shallow zone and implies convergence of two plates covered with continental crusts. It may be emphasized that, excepting those of Hindukush and Arakan, all Himalayan earthquakes originated at vary shallow depths of less than or about 50 km, and there is no evidence of the tendency for increasing depths northwards (Valdiya 1976).

Significantly in the Bundelkhand-Faizabad and Manger-Saharasa ridges, which are in all probability tectonically and seismologically inactive, there is practically no or only very feebly seismicity in Nepal. This may be interpreted as northeasterly extension into the Himalaya of the seismically

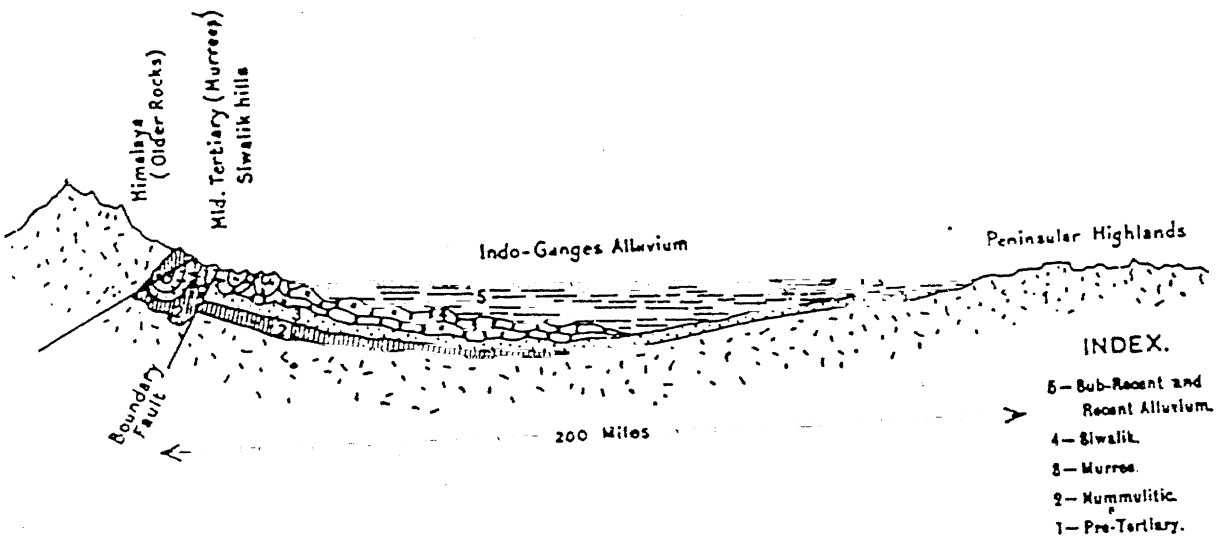

Fig. 2.5 Diagrammatic section of possible sequence within the Indo-Gangetic trough

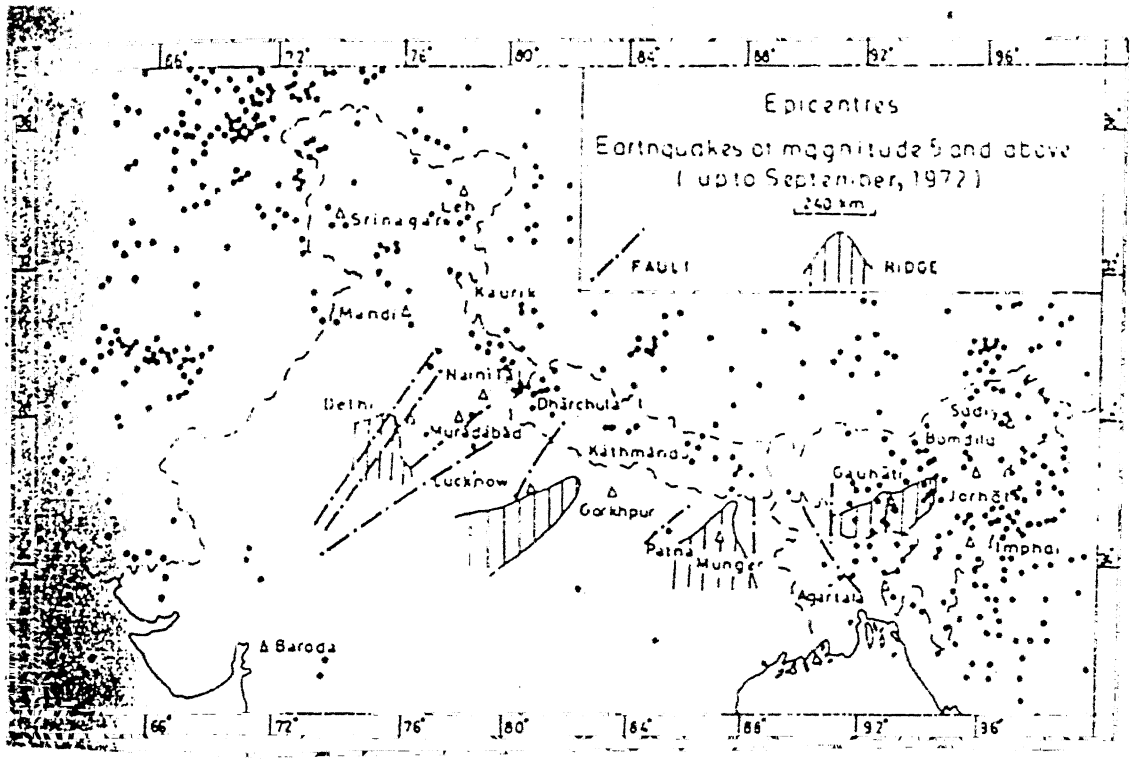

Fig. 2.6 Distribution of epicentres of earthquakes of magnitude 5 and above upto September 1972

inactive ridges of the Ganga basin. The high seismicity of the Ganga basin is also attributed to the movement of different blocks of Indian plate with different speeds and directions.

2.4 SEISMICITY OF PENINSULAR INDIA

Until recently, the peninsular shield, covering about one third of the Indian sub-continent, has been considered relatively free from earthquakes (Richter 1958). Until 1967, only three earthquakes of some consequence with a maximum intensity of VII on Modified Mercalli (M.M.) scale have been reported. These occurred at Mahabaleshwar (1764), Bellary (1843) and Coimbatire (1900). Recent earthquake occurrences at Koyana (1967), Bhadrachalam (1969) and Broach (1970), in a short span of time, have raised doubts about the aseismic nature of the region (Figure 2.7).

2.4.1 TECTONIC FEATURES OF THE INDIAN PENINSULA

The basement is formed by Archean gneisses, schists and igneous rocks, which have been metamorphosed to various degrees. They are exposed in the southern, eastern and northern parts of peninsula, occupying two thirds of its territory (Figure 2.8). The structure of peninsula is often referred to as the Precambrian shield.

There are four regional trends of folds in the Archean rocksin the different parts of peninsula,

(i) the Dharwarian folds of NNW-SSE and meridional strike; they are in the central and south - eastern parts of peninsula,

(ii) eastern Ghats folds of NE-SW strike; they are in the southern and eastern parts of peninsula,

(iii) the Satpura folds of WSW-ENE strike; they are in the

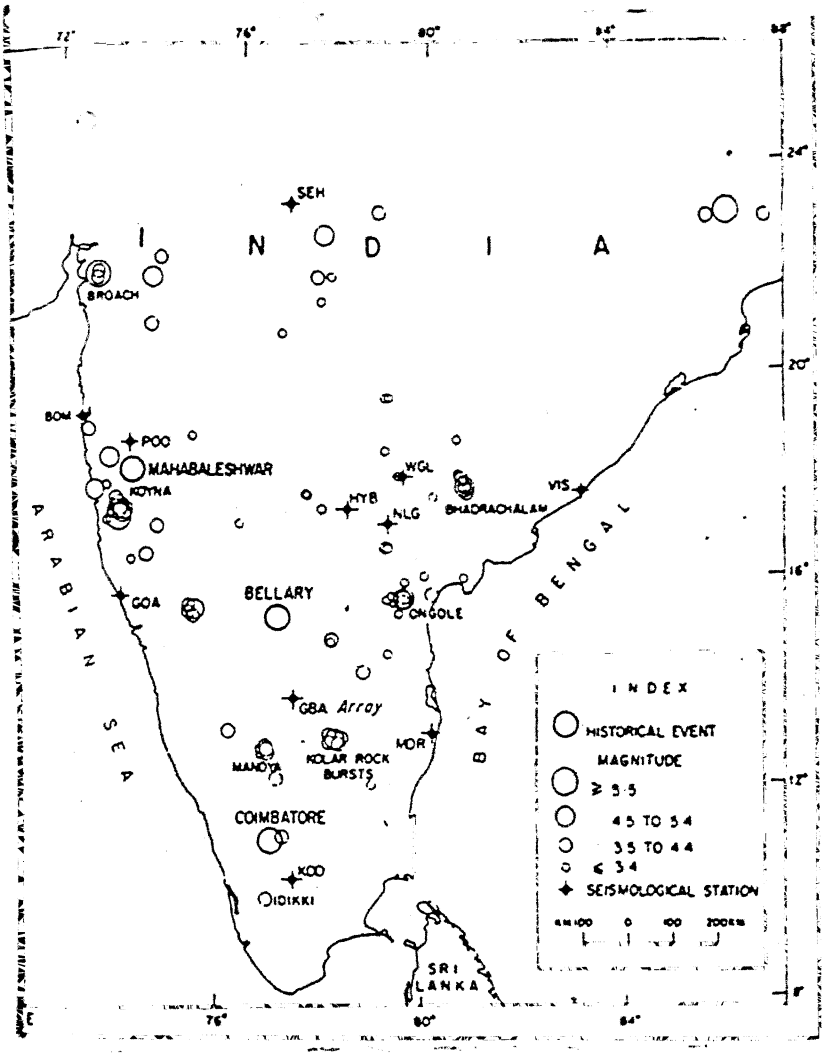

Fig. 2.7 Map showing the locations of epicentres in Indian Peninsular region

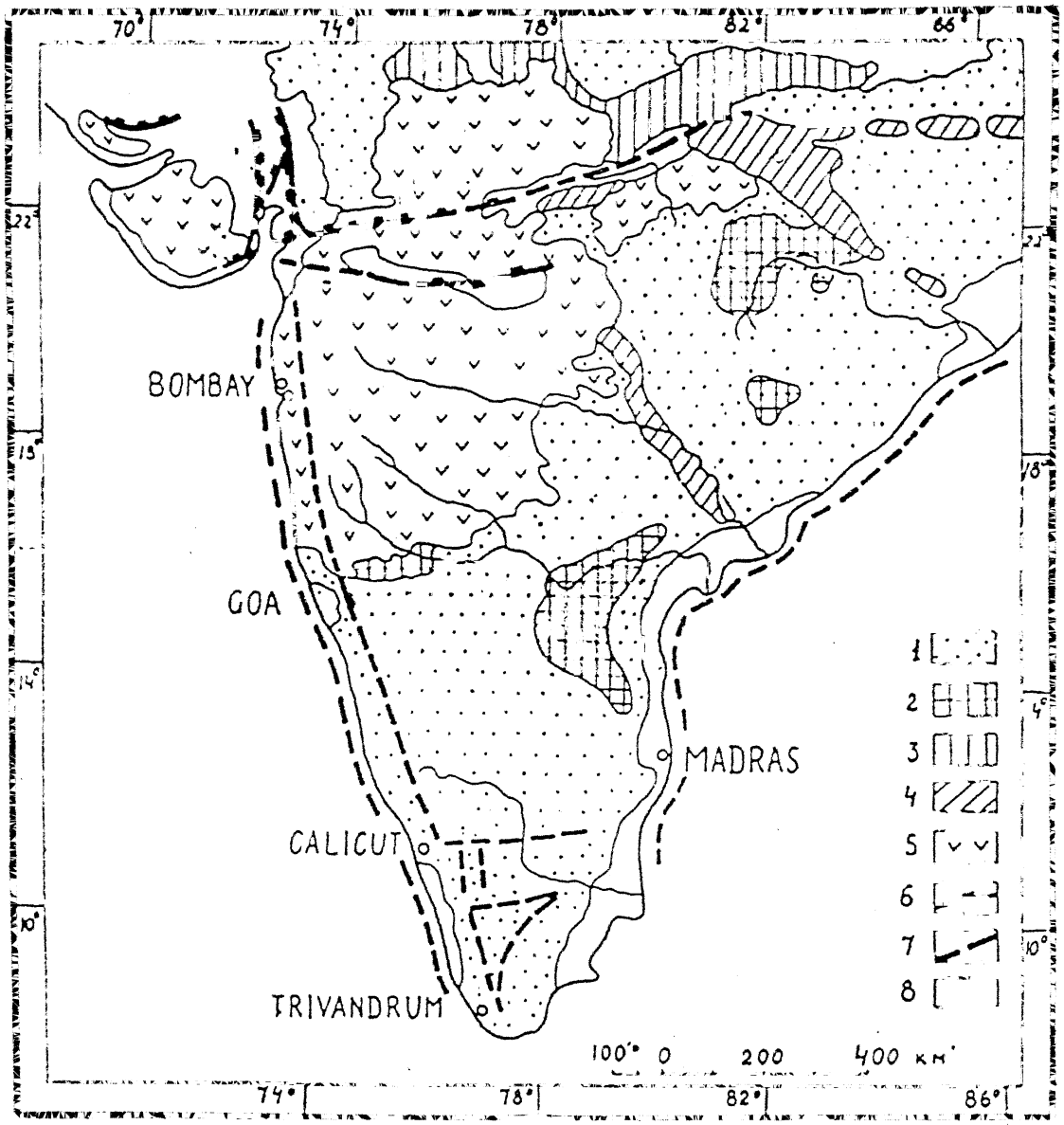

Figure 2.8 Tectonic map of Indian Peninsula

1—the basement rocks of Indian platform ; 2-5—the layers of cover of Indian platform ; 2—Cuddapah sediments ; 3—Vindhyan; 4—Gondwanyan; 5—Deccan traps ; 6—the zone of tertiary faults, which is established ; 7—the zone of tertiary faults, which is supposed to exist ; 8—quarternary sediments mostly.

northern and east-northern parts of peninsula, and

(iv) the Aravalli folds of NE-SW strike; trend from Aravalli range towards Delhi.

Seismicity in the Koyana region of Indian peninsula increased considerably following the impounding of the Koyana reservoir in 1962. A detailed examination of the foreshock - aftershock pattern and source dynamics of the earthquakes in this region Gupta et al. 1969,1971) showed different characteristics from those of the earthquake sequence in the Godavari valley, which belongs to peninsular India (Gupta et al. 1970). The above discussion shows that the seismicity of peninsular India is increased after the impounding of the major reservoirs like Koyana, Nagarjuna Sagar and various others. The continued seismic activity in the vicinity of the Koyana Dam in the peninsular shield of India after impoundment of the Shivaji Sagar Lake, is a well-known example of man-made reservoir-induced seismicity.

2.5 SEISMIC ZONING OF INDIA

Millions of people have died and property worth crores of rupees has been destroyed by earthquakes. According to the 1965 Seismo-security Report of UNESCO during the period 1926 to 1950, over 3,50,000 people were killed and damage to construction totalled to about ten thousand million dollars.

Some of the great earthquakes of the world have occurred in India. For example the Assam earthquake of 1897 was felt over an area of 1,750,000 sq miles, Kangra earthquake of 1905 claimed over 20,000 lives, Bihar-Nepal earthquake of 1934 claimed over 10,000 lives etc. Considering the losses India has suffered from earthquakes, it is imperative that Indian earthquakes be

thoroughly investigated for appropriate seismic zoning of India.

Tandon (1953) prepared first seismic zoning map of India which is shown in Figure 2.9. In this map, India has been broadly divided into three regions viz, foothills of Himalayas, Indo-Gangetic basin and Peninsular shield. Foothills of Himalayas from Kashmir valley to Assam and Burma are depicted to be liable to severe damage. Indo-Gangetic plain, Kutch etc. come under regions of moderate damage and Peninsular shield is shown to correspond to regions of minor or no damage. Guha (1962) modified the map given by Tandon (1953) and divided India into five zones, numbering from 0 to 4 and maximum expected intensities ranging from IV and below to IX and above on the Modified Mercalli scale were allotted to these five zones. We have reproduced the map in Figure 2.10 given by Guha (1962). In 1962, Indian Standards Institution in their recommendations for earthquake resistant design of structures (IS:1893-1962) published a seismic zoning map of India and increased the number of zones to 7 (Figure 2.11). The design earthquake acceleration of 0 for hard soil in zone number 0 and 0.12g for soils in zone number VI were adopted. This was because of the fact that acceleration attenuation is rapid in hard soils.

The seismic zoning map of Indian Standard Institution was revised in 1966 to incorporate the additional seismic data collected in India and experience gained since the earlier publication of 1962. Like the earlier map (Figure 2.11) this map (Figure 2.12) also show seven zones but the seismic coefficients have been increased for most of the regions and were specially notable in the Peninsular shield.

However, in all the above seismic zoning maps prepared for

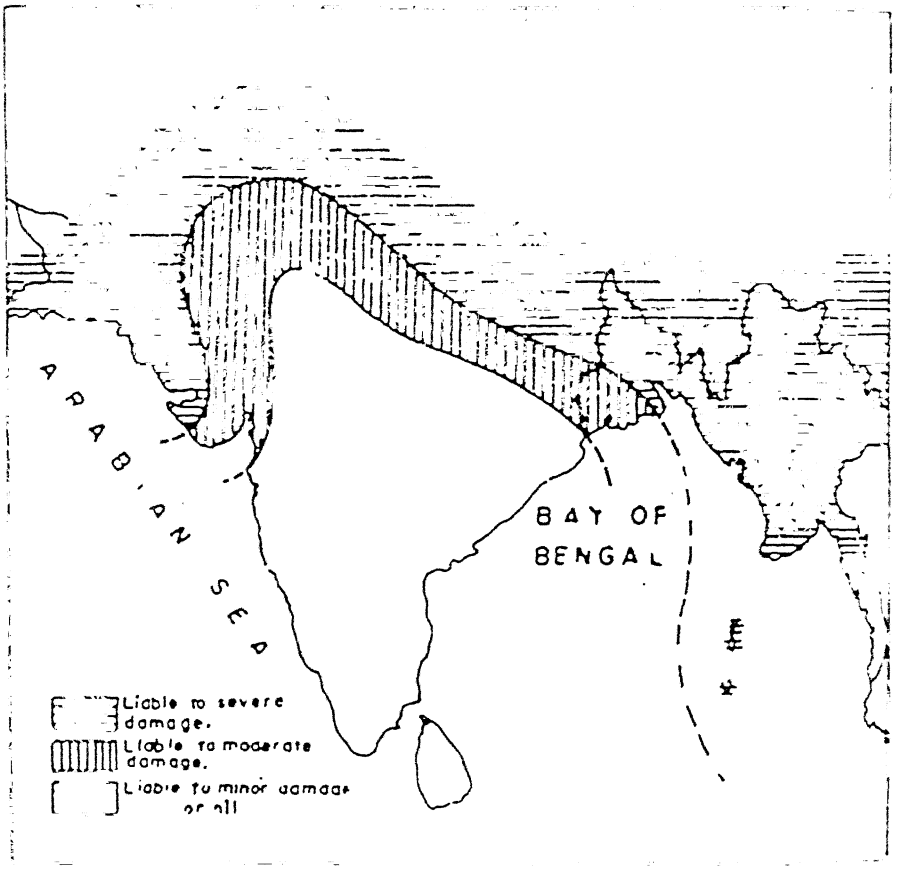

Fig. 2.9 Seismic zoning map of India (Tandon 1953)

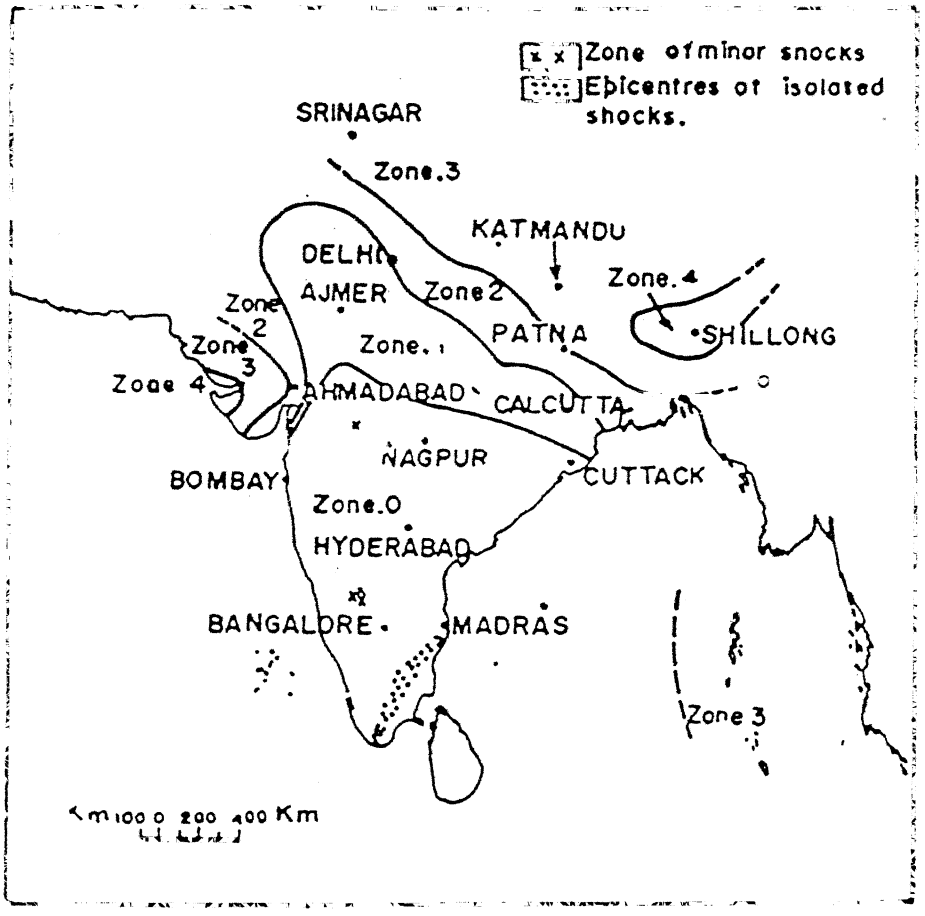

Figure 2.10 Seismic regionalisation map of India (Guha 1962)

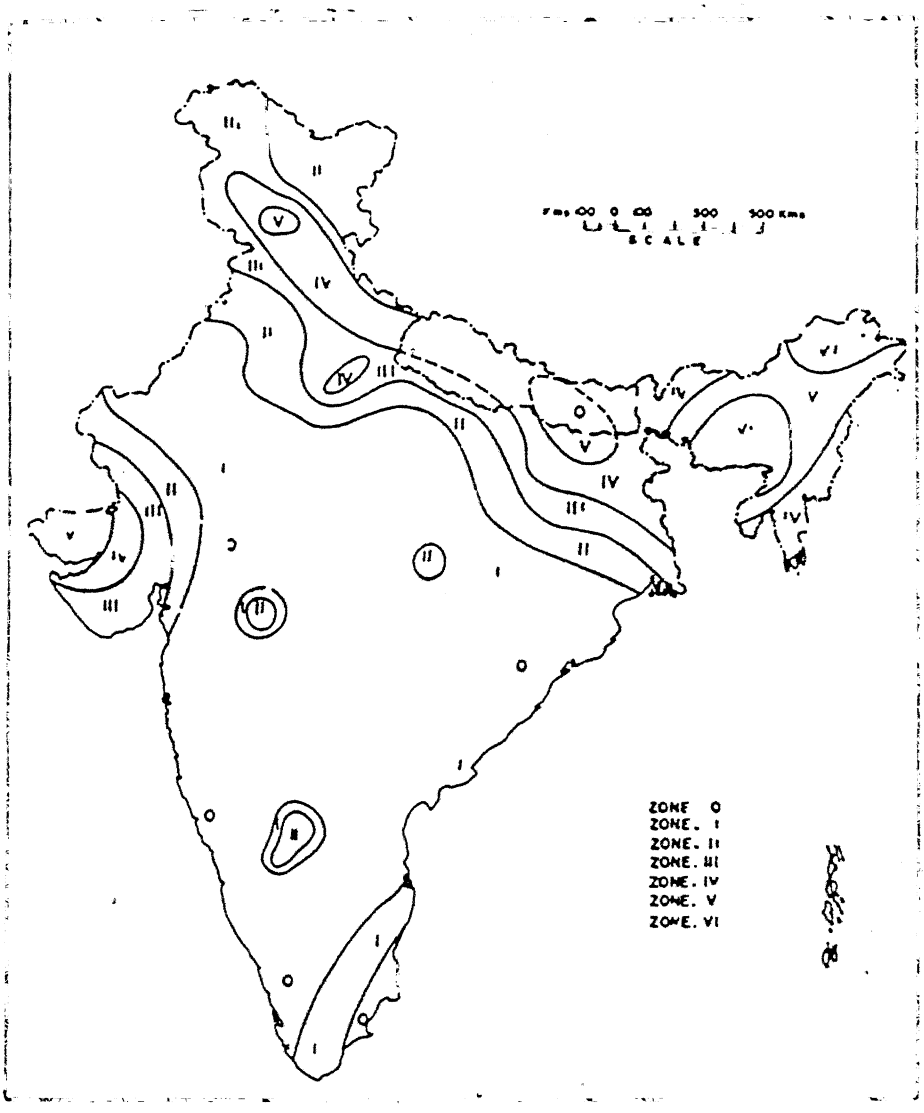

Fig. 2.11 Map of India showing seismic zones
(I: S. I. 1962)

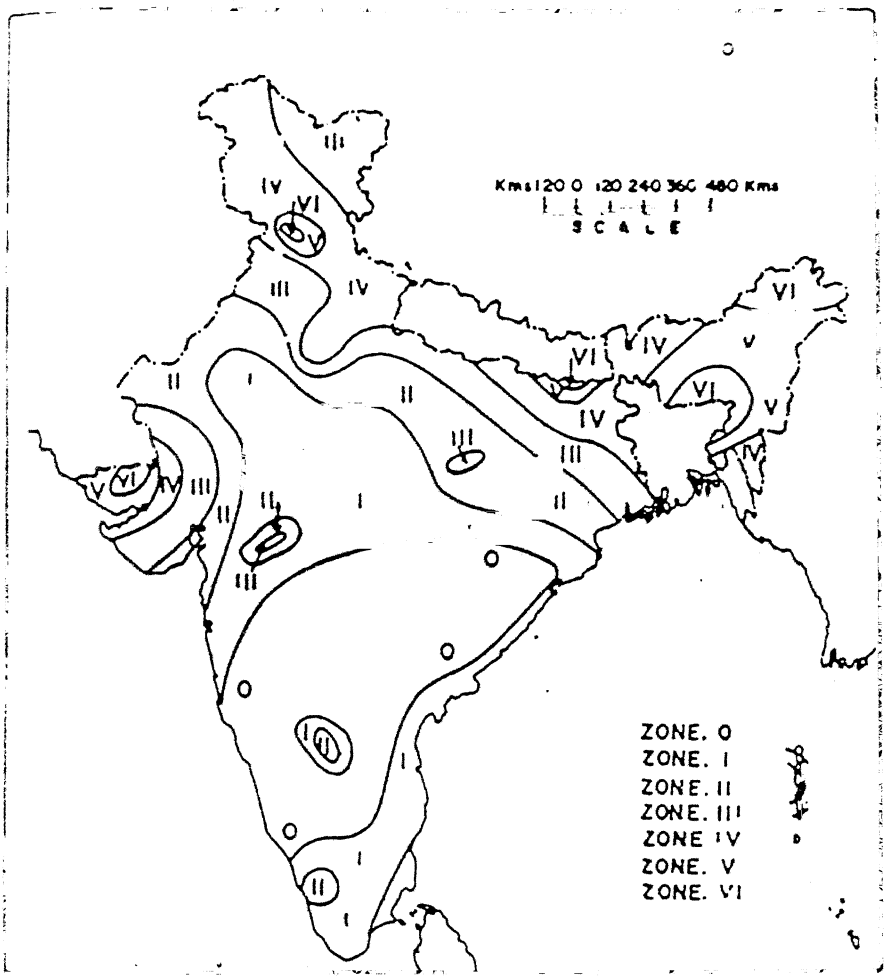

Fig. 2.12 Map of India showing seismic zones
(I. S. I. 1966)

India, the Peninsular shield was considered to have no or little seismicity, but it experienced the Koyana earthquake of magnitude 6.3 on December 10,1967. This earthquake has been preceded and followed by hundreds of earthquakes during 1962 to 1967. Some of them are of magnitude of the order of 5.0. In 1968, Gubin prepared a multiple element seismic zoning map for the Peninsular India, using the data collected from the Koyana earthquake (Figure 2.13).

Figure 2.13 has been based on the tectonic differential movements and deformation of the Indian platform. The deformation causes accumulation of strain in the earth's crust and subsequent earthquake occurrences (Gubin 1968). The seismogenic zones depicted on the map are said to include the areas of recorded shocks and the areas within which they have not yet recorded but may arise in future, in accordance with tectonic considerations.

IS: 1893 has been revised in 1970 and further in 1975 to incorporate Gubin's recommendations and recent seismicity. The following changes have been incorporated in the third revision of IS: 1893

(i) the standard incorporated seismic zone factors on a more rational basis and

(ii) importance factors have been introduced for various structures.

The seismic zoning map of India is once again revised in 1984 (IS: 1893-1984). It is important to note that the seismic coefficient, used in the design of any structure, is dependent on many variable factors and it is an extremely difficult task to determine the exact seismic coefficient in each given case. In IS: 1893-1984 a seismic zoning map (Figure 2.14) is included which divides the country into five zones depending on the seismicity.

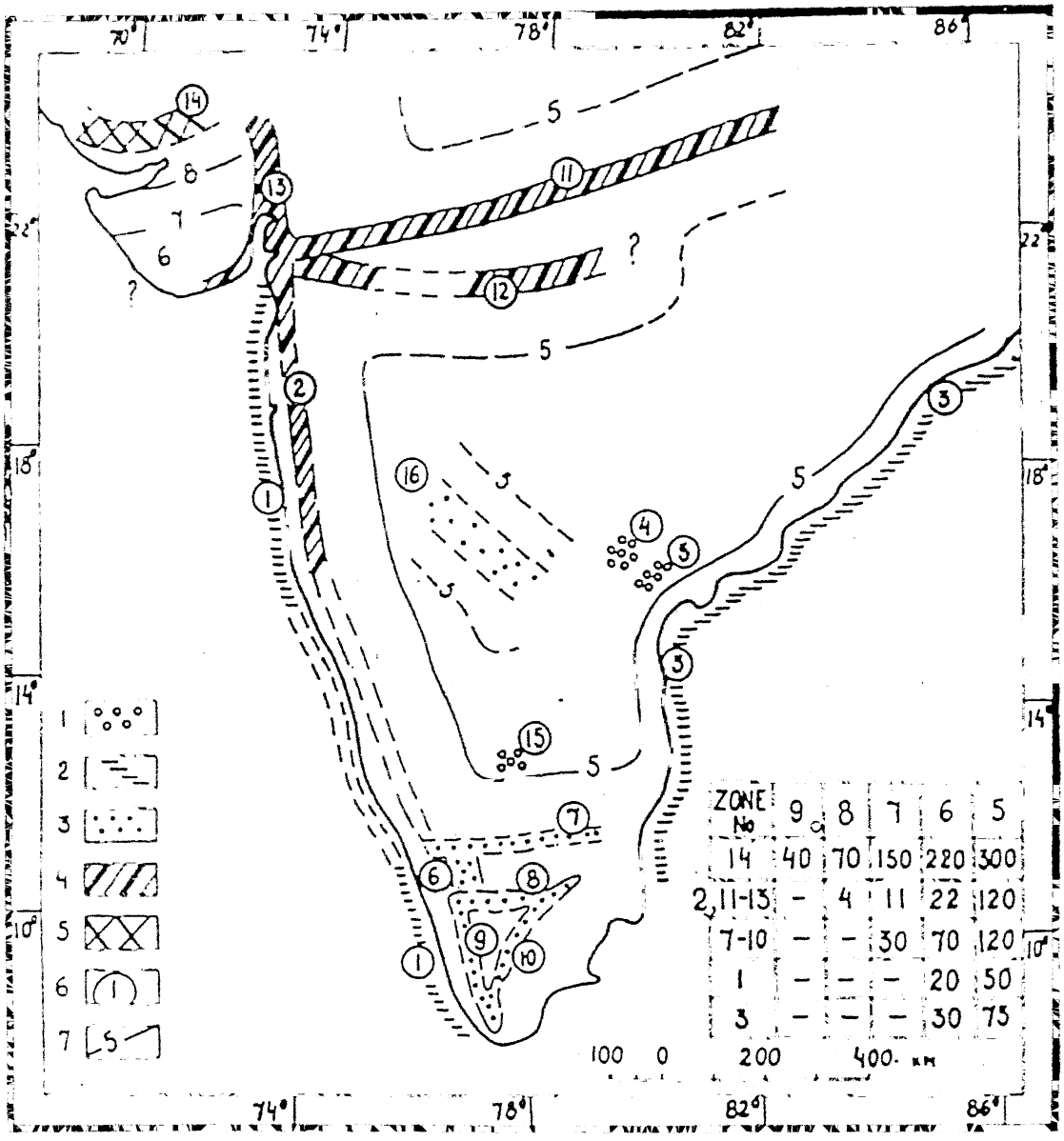

Fig. 2.13 Map of seismic zoning of Indian Peninsula (Gubin 1968)

1-5—the zones in which earthquakes may arise of maximum intensity in the epicentre: 1-of intensity 5; 2-of intensity 6; 3-of intensity 7; 4-of intensity 8; 5-of intensity 9 and more; 6-number of the zone, ; 7-the boundary to which may reach the intensity of given grade, from the possible maximum earthquakes of the neighbouring seismogenic zone. The table on the map shows the expected intensity distribution of possible maximum earthquakes beyond this seismogenic zone. In the table, the top row-intensity grades; columns-distances in kilometers from respective seismogenic zone (first column).

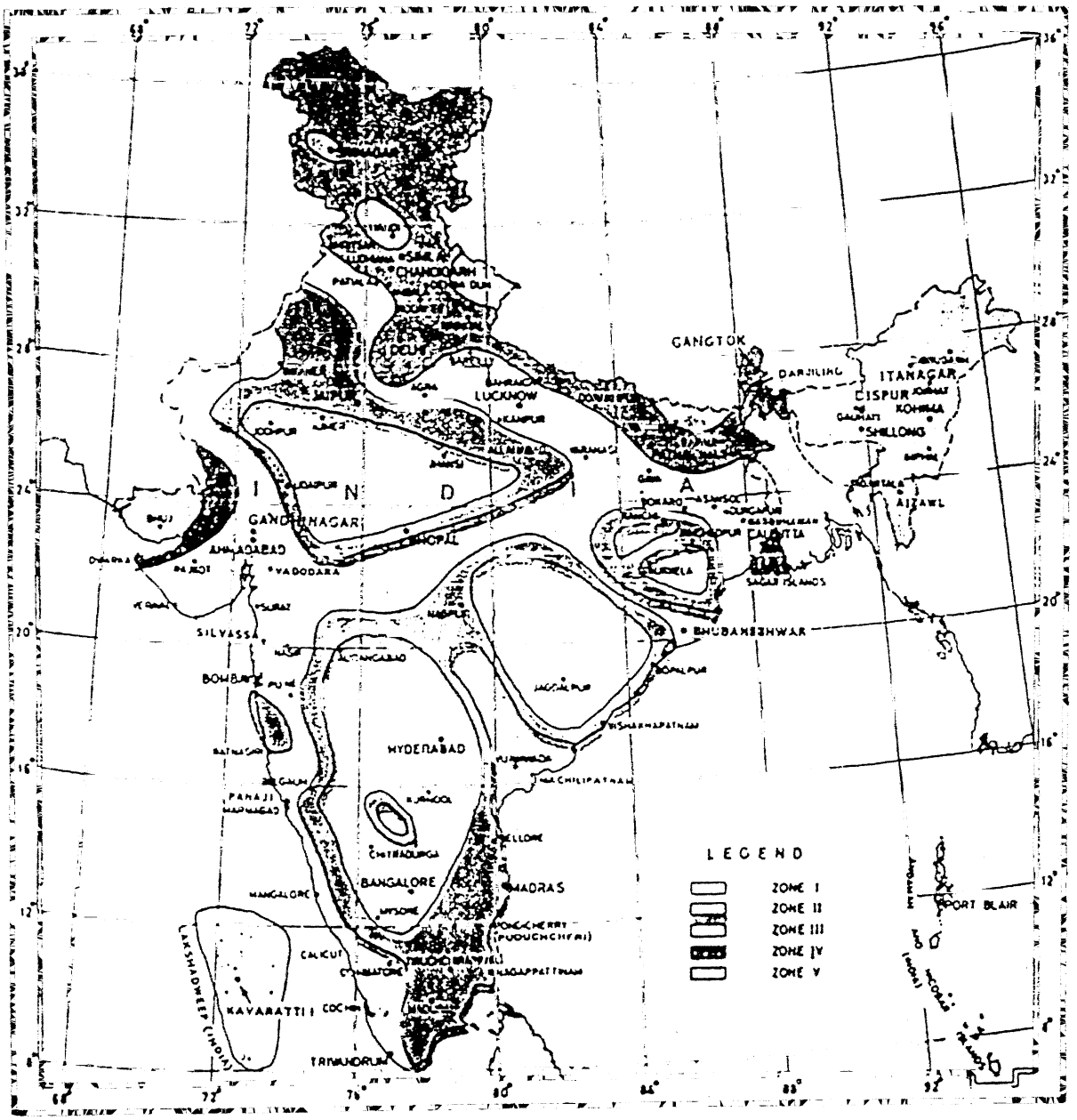

Fig. 2.14 Map of seismic zoning of India
(I. S. I. 1984)

The object of this map is to classify the area of the country into a number of zones in which one may reasonably except earthquake shock of more or less same intensity in future. The Modified Mercalli Intensity (M.M.I.) broadly associated with the various zones is V or less, VI, VII, VIII and IX and above for zones I, II, III, IV and V, respectively.

Most of the seismic zoning maps prepared for India comes under the category of single element maps, which show the maximum intensity of earthquakes likely to occur at each point within the area covered by the map. Statistical analysis carried for the number and intensity of earthquakes actually recorded in the area is the base of such maps and besides the seismograph data, historical descriptive records are also some times made use of. In the present study, we have proposed the attenuation relations for strong ground motion in India based on the data collected from the recently installed strong motion accelerographs. The intensity attenuation together with strong ground motion attenuation, it is possible to assess the seismic risk of a region more precisely. The seismic zoning maps which have been developed in the absence of knowledge of attenuation of strong seismic ground motion should be revised from time to time based on the latest data and also in view of the latest geological information.

CHAPTER III

ATTENUATION CHARACTERISTICS OF SEISMIC GROUND MOTION

3.1 INTRODUCTION

For various engineering and scientific purposes, it is desirable to estimate the maximum accelerations at various locations during earthquakes. Maximum accelerations are generally higher for higher magnitude earthquakes and depends on the earthquake magnitude. The peak acceleration decreases with epicentral distance i.e., the distance from the zone of energy release. The relationship between maximum acceleration and distance from zone of energy release has been called an attenuation curve for maximum acceleration. In this Chapter we have discussed the attenuation characteristics of strong ground motion.

3.2 ATTENUATION IN ROCK FORMATIONS

Prior to San Fernando earthquake of 1971, only very few rock motions with maximum acceleration exceeding 0.1g has been recorded during earthquakes.

The attenuation of the amplitude of acceleration with distance from the fault for a given motion is due to two different mechanisms (Schnabel et al. 1973). The first mechanism deals with geometric attenuation. This attenuation is the decrease in specific energy as the wave propagates outward and occupies a large volume. This geometric attenuation is a function of the geometry of the fault relative to the geometry of the wave front. The second factor in the attenuation is the absorption of energy caused by the internal damping in rock. This attenuation is in

general found to increase linearly with the frequency, resulting in a more rapid attenuation of the higher frequency components. The damping is much higher for softer rocks and soils compared to the base crystalline rock.

A method for predicting the total attenuation of rock motions as a function of distance from the source can be based on the above general concepts, as summarized below:

(i) the total attenuation is the result of geometric spreading and internal damping in the rock,

(ii) the energy is released simultaneously over the whole fault break, and is distributed uniformly over the the fault break and the progressive wave front,

(iii) the energy is mainly carried by body wave travelling in the base crystalline rock and the waves are refracted in to a near vertical path near the surface,

(iv) the distance to the nearest point on the fault break is the primary geometric factor determining the attenuation as a result of damping in rock, and

(v) earthquake record may be represented by a series of harmonic motions.

3.3 ATTENUATION RELATIONS FOR PEAK ACCELERATION AND VELOCITY

Esteva (1970) has studied a number of United States earthquakes and proposed the following relation for particle velocity:

$$\log v = 1.18 + 0.54M - 1.7 \log (R + 0.17 e^{0.57+M}) \quad ...(3.1)$$

where v is the ground velocity (cm/sec), R is the focal distance (km), and M is the magnitude.

Ambraseys (1972, 1973a, 1973b) determined the relationship that gives velocity as a function of M.M. intensity (MMI) scale, for San Fernando earthquake of February 9, 1971. He found a large dispersion in the data collected and also found that correlation between MMI and acceleration, velocity, or displacement are very poor. The relations proposed by Ambraseys have been given in Table 3.1.

Espinosa (1977) has studied the particle-velocity attenuation relations for San Fernando earthquake of Feb 9, 1971. Espinosa (1971) has determined the attenuation of particle velocity obtained from the first integration of the accelerograms recorded during the San Fernando, California, earthquake of Feb 9 1971. The accelerograms obtained at 61 stations in the San Fernando valley and neighbouring regions have been used to derive a number of parametric equations for use in the determination of the seismic parameters for structural design including that for nuclear reactors.

The attenuation of the average value of the particle velocity (V), as a function of distance (Δ) , is given as

$$\log V = 3.19 - 1.35 \log \Delta \qquad \ldots(3.2)$$

The attenuation of Modified Mercalli intensity (I) with distance (Δ) and the horizontal particle velocity (v) are given as

$$\log \Delta = 3.05 - 0.25\ I \qquad \ldots(3.3)$$

$$\log v = -0.93 + 0.29\ I \qquad \ldots(3.4)$$

Attenuation relations with the horizontal velocity (v^H)and vertical velocity (v^H) are given as

$$\log v^{H} = 3.68 - 1.35 \log \Delta \quad \ldots(3.5a)$$

$$\log v^{V} = 2.91 - 1.03 \log \Delta \quad \ldots(3.5b)$$

Empirical relations between ground velocity and other parameters have been given by different authors which are summarized in Table 3.1.

TABLE 3.1

$\log v = 1.18 + 0.43M - 1.7 \log(R+0.17\, e^{0.57+M})$	Esteva (1970)
$\log v = 2.17 + 0.55M - 1.5 \log R$	Mickey (1971)
$\log v = -0.98 + 0.72M - 0.5\log(11.5M-53) - \log R_0$	Ambraseys (1972)
$\log v = 0.3\ I - 1.16$	Ambraseys(1973b)
$\log v^{H} = -0.18 + 0.26\ I$	Ambraseys(1973a)
$\log v^{H} = -0.63 + 0.25\ I$	Trifunac and Brady (1975)
$\log v^{V} = -1.10 + 0.28\ I$	Trifunac and Brady (1975)

Where, I is M.M intensity rating, M is magnitude, R is focal distance, v is ground velocity, and the superscripts H and V refer to horizontal and vertical components.

Orphal and Lahoud (1974) have studied the prediction of peak ground motion resulting from earthquakes and nuclear explosions. A statistical analysis shows that the peak horizontal accelerations recorded from San Fernando earthquake attenuate with focal distance as $R^{-1.39}$. This attenuation rate is found to be nearly identical to that reported for peak accelerations from underground nuclear explosions and it has been assumed that the derived attenuation is independent of source parameters. They also scaled the earthquake peak velocity and displacement with magnitude, assuming that the attenuation of peak velocity and displacement are identical for earthquakes and underground nuclear explosions.

The equations resulted from the analysis are given below.

$$a = 6.60 \times 10^{-2}\ 10^{0.4M}\ R^{-1.39} \qquad \ldots(3.6)$$

$$v = 7.26 \times 10^{-1}\ 10^{0.52M}\ R^{-1.34} \qquad \ldots(3.7)$$

and $$d = 4.71 \times 10^{-2}\ 10^{0.57M}\ R^{-1.18} \qquad \ldots(3.8)$$

where a,v and d are maximum acceleration (g), velocity (cm/sec) and displacement (cm) respectively, M is the local magnitude and R is the focal distance (km). In this, no attempt has been made to account for effects of geology at recording sites.

Murphy and Lahoud (1969) demonstrated that the peak ground motion from nuclear explosions could be adequately described by an equation of the following form,

$$A = k\ W^n R^m \qquad \ldots(3.9)$$

where A is the ground motion amplitude, W is the explosion yield, R is the focal distance, and k, n and m are constants determined by regression analysis. It has been assumed that nuclear explosion yield and magnitude, M are related by an equation of the form

$$M = \alpha + \beta\ (\log W) \qquad \ldots(3.10)$$

where α and β are constants.

The functional form that has been assumed to relate peak earthquake ground motion amplitude (A), to magnitude and focal distance has been derived by combining equations (4.9) and (4.10) as

$$A = \lambda\ 10^{\alpha M}\ R^{\beta} \qquad \ldots(3.11)$$

where λ, α and β are constants.

On the other hand, many researchers have suggested that earthquake intensity is best related to peak velocity. A commonly used equation relating intensity (I) and peak velocity (v) is given as (Newmark and Rosenblueth 1971)

$$I = \log \left(\frac{14\ v}{\log 2} \right) \qquad \ldots(3.12)$$

Substituting v from equation (3.7)

$$I = 3.3 + 7.74\ M - 4.45 \log R \qquad \ldots(3.13)$$

Assuming focal depth R = 15 km,

$$I_o = 1.74\ M - 1.95 \qquad \ldots(3.14)$$

This equation compares well with the empirical relation

$$I_o = 1.5\ M - 1.5 \qquad \ldots(3.15)$$

reported by Gutenberg and Richter (1956).

Murphy and Obrien (1977) have given the acceleration/intensity correlation using a world wide data sample from data measured from nearly 1500 strong ground motion acclerograms. It has been found that the correlation equation relating peek horizontal ground acceleration (a), to Modified Mercalli Intensity (I) as

$$\log a = 0.25\ I + 0.25 \qquad \ldots(3.16)$$

for 'a' given in cm/sec^2. It has also been shown that the correlation on other variables such as local earthquake magnitude (M), epicentral distance (R), and the geographical region in which the earthquakes are occurring, as

$$\log a = 0.14\ I + 0.24\ M - 0.68 \log R + \beta \qquad \ldots(3.17)$$

where 'R' is given in km. and

$$\beta_{\text{western United States}} = 0.60 \qquad \ldots(3.18)$$

$$\beta_{\text{Japan}} = 0.69 \qquad \ldots(3.19)$$

$$\beta_{\text{Southern Europe}} = 0.88 \qquad \ldots(3.20)$$

Kaila and Sarkar (1978) have studied the intensity and epicentral correlations for different earthquakes in different directions and have given the following relation,

$$\frac{I}{I_0} = \text{EXP}\ \{\ -(1.5616/h^2 + 0.0011)\ \Delta\ \} \qquad \ldots(3.21)$$

for $15 \leq h \leq 240$ km where h and Δ are in km, which represents earthquake intensity attenuation pattern with epicentral distance (Δ) and focal depth (h). It has also been proposed that the maximum intensity (I_o), the magnitude (M), and the focal depth (h), of an earthquake are empirically related as

$$I_o = 1.5\ M - 4.5 \log h + 4.5 \qquad \ldots(3.22)$$

where $8 \leq h \leq 70$ km.

Hasegawa et al. (1980) have proposed a relation for the attenuation of strong ground motion for Canada based on the data obtained from the United States. The proposed relations for western Canada are given as (Hasgawa et al. 1980)

$$a_p(\text{cm sec}^{-2}) = 10\ e^{1.3M}\ R^{-1.5} \qquad \ldots(3.23)$$

$$v_p(\text{cm sec}^{-1}) = 0.0004\ e^{2.3M}\ R^{-1.3} \qquad \ldots(3.24)$$

and for eastern Canada,

$$a_p(\text{cm sec}^{-2}) = 3.4\ e^{1.3M}\ R^{-1.1} \qquad \ldots(3.25a)$$

$$v_p(\text{cm sec}^{-1}) = 0.00018\ e^{2.3M}\ R^{-1.0} \qquad \ldots(3.25b)$$

where a_p, v_p, M and R stand for horizontal peak acceleration, horizontal peak velocity, magnitude and hypocentral distance (km.), respectively. Hasegawa et al. (1980) have adopted the following attenuation model proposed by Kanai (1961).

$$\log AGM = b_1 + b_2 M - b_3 \log R \qquad \ldots(3.26)$$

where, AGM is amplitude of ground motion, M is the magnitude, R is the distance from the focus, and b_1, b_2, and b_3 are constants which depend on conditions of subsurface.

Sabetta and Pugliese (1987) have derived relations for the attenuation of peak horizontal acceleration and velocity from Italian strong motion records. They have analysed the data of accelerogram records for the earthquakes of magnitudes 4.6 to 6.8, and the resulting relations are (Sabetta and Pugliese 1987)

$$\log A = -1.562 + 0.306\ M - \log(R^2 + 5.8^2)^{0.5} + 0.169\ S \qquad \ldots(3.27)$$

$$\log V = -0.710 + 0.455\ M - \log(R^2 + 3.6^2)^{0.5} + 0.133\ S \qquad \ldots(3.28)$$

where A is peak horizontal acceleration in g, V is peak horizontal velocity in cm/sec, M is magnitude, R is the closest distance to the surface projection of the fault rupture in km and S is a variable taking the value of 0 and 1 based on the geology of local sites.

The ground motion model adopted for the above work for modelling the attenuation is represented by the functional form as

(Sabetta and Pugliese 1987)

$$F(y) = a + F_1(M) + F_2(R) + F_3(S) + \psi \qquad \ldots(3.29)$$

where y is the predicted strong motion parameter, $F_1(M)$ is a function of magnitude, $F_2(R)$ is a function of distance, $F_3(S)$ is a function taking into consideration of the site effect and ψ is a variable representing uncertainty in y.

Comparing the attenuation relations (equations 3.27 and 3.28) for peak horizontal acceleration and peak horizontal velocity, (Sabetta and Pugliese 1987) it has been found that,

(i) the magnitude dependence is higher for peak horizontal velocity than for peak horizontal acceleration, whereas the value of the additive constant to R^2 is lower for peak horizontal velocity,

(ii) the effect of site geology is slightly lower for peak horizontal velocity than for peak horizontal acceleration,

(iii) the goodness of fit is better for peak horizontal acceleration than for peak horizontal velocity.

Taheri and Anderson (1988) have interpreted the 1978 Tabas, Iran, earthquake strong motion data using the following attenuation relations.

$$\log P = \alpha - \beta \log R - \gamma R \qquad \ldots(3.30)$$

and

$$R = (\Delta^2 + h^2)^{0.5} \qquad \ldots(3.31)$$

where P is the peak value of the ground motion parameter, Δ is the nearest distance to fault surface, h compensates for energy release occurring away from the nearest point on the fault surface, and α, β, and γ are parameters which depend on the

;eology of the local sites. The coefficients adopted by Taheri and ınderson (1988) have been shown in Table (3.2).

TABLE 3.2

correlation	units	α	β	γ	h (km)
peak acc.	cm/sec^2	3.40	0.64	0.0025	7.3
peak vel.	cm/sec	2.31	0.55	0.0025	4.0

Abrahamson and Litehiser (1989) have studied the attenuation of peak vertical acceleration from the data collected from 76 worldwide earthquakes using an attenuation model that has a magnitude dependent shape. The proposed relation is given as

$$\log a_v(g) = -1.15 + 0.245\ M - 1.096 \log (R + e^{0.256M}) + 0.096\ F - 0.0011\ ER \quad ..(3.32)$$

where M is magnitude, R is the distance in km to the closest approach of the zone of energy release, F is a dummy variable that is 1 for reverse or reverse oblique events and 0 for intraplate events. They have also proposed the following relation for peak horizontal acceleration

$$\log a_v(g) = -0.62 + 0.177\ M - 0.982 \log (R + e^{0.284M}) + 0.132\ F - 0.0008\ ER \quad ..(3.33)$$

The expected ratio of vertical to horizontal strong motion predicted by these equations is two-thirds for earthquakes with magnitude less than 7.0 and distances greater than 20 km. The expected ratio exceeds 1.0 for earthquakes with magnitude greater than 8.0 at very short distances.

Campbell (1989) has studied the dependence of peak horizontal acceleration on magnitude, distance and site effects for small-

magnitude earthquakes in California and its surrounding regions, and the proposed relation is given as

$$\ln (PHA) = -2.501 + 0.623\ M - \ln (R+7.28) + \psi \qquad ...(3.34)$$

where PHA is the mean of the two horizontal components of peak acceleration in g, M is the local magnitude, R is epicentral distance in km and ψ is random error term with mean of zero and standard deviation of 0.506.

The attenuation model adopted for developing the above relation is

$$\ln (PHA) = \alpha + \beta\ M + \delta \ln (R + c_1\ EXP(c_2 M)) + f(H) + \psi \qquad ..(3.35)$$

where H and M are focal depth in km and magnitude respectively, and α, β, δ, c_1 and c_2 are constants.

Joyner and Boor(1982,1988) have developed the following equations for estimating horizontal ground motion from shallow earthquakes in western North America:

$$\log y = \alpha + \beta\ (M - 6) + \gamma\ (M - 6)^2 + \delta \log R + k\ R + S \qquad ..(3.36)$$
$$5.0 \leq M \leq 7.7$$

$$R = (R_0^2 + h^2)^{0.5} \qquad ...(3.37)$$

where y is the predicted ground-motion, M is the moment magnitude of the earthquake, R_0 is the shortest distance(km) from the site of fault rupture on the surface of the earthquake, and S is the site-effect coefficient. Values of α, β, γ, δ, k, h and S for soil sites (sites with 5 m or more of soil), determined by fitting the strong-motion data set, are given in Table 3.3 for estimating quantities corresponding to the randomly oriented horizontal component. S=0 has been taken for rock sites.

TABLE 3.3

Peak acceleration (g)					
α	β	γ	δ	h	S
0.43	0.23	0.0	-1.0	8.0	0.0
Peak Velocity (cm/sec)					
α	β	γ	δ	h	S
2.09	0.49	0.0	-1.0	4.0	0.17

CHAPTER IV

RESULTS AND DISCUSSIONS

4.1 INTRODUCTION

The attenuation of strong ground motion depends on the source parameters, type of fault and subsurface layer parameters. In developing relationships for estimating ground motion the main factors considered are earthquake magnitude, intensity, source distance and local geological conditions. Many workers also include type of faulting and fault length. Because the effect of various factors which improve the estimation of ground motion has not been fully understood. The attenuation relationships are developed by the correlation of observed ground motion data, the ground motion estimates and the estimates of variability will implicitly reflect these additional factors. Strong ground motion instruments are deployed in a quasi-random fashion in earthquake prone regions in order to find out the effect of ground motion on the structures.

In general, earthquake safety analyses require prediction of ground motion at a particular site for an earthquake of specified magnitude and hypocentral distance. Ideally, the predicted ground motion is in the form of a complete seismogram from which peak ground motion values at a seismological observatory, are obtained. Peak ground acceleration, Peak ground velocity and Intensity data have traditionally been used by the seismological and engineering communities to characterize strong ground motion.

We have derived a set of empirical relations for predicting Peak horizontal ground acceleration and peak horizontal velocity, which has been used to study the attenuation characteristics of

strong ground motion of various regions in India. We have used the Isoseismal maps of major earthquakes and have studied the variation of Intensity with the epicentral distance.

4.2 ACCELERATION AND VELOCITY DATA

For the present study, we have taken strong ground motion data (Chandrasekaran and Das 1988) of five different earthquakes, which have been recorded by the strong motion accelerographs installed in the seismic zones IV and V covering Himalaya and Himalayan foothills. Among these five events one is recorded by Kangra array and the rest four events are recorded by Shillong array. These records have been analysed and strong ground motion characteristics of these events have been discussed. These are the first records from the Himalayan region which are of interest to the Engineers and Scientists working in India and abroad.

The Kangra array registered an event on April 26, 1986, which was the only significant activity so far of Magnitude 5.7. The four events registered by Shillong array are: September 10, 1986 of magnitude 5.7, May 18, 1987 of magnitude 5.7, February 6, 1988 of magnitude 7.2. Shillong region is more active, and even in the short span of time, has produced valuable data. The data of these events are given in Table 4.1. In this Table we have shown the hypocentral distances for each recording station which have been calculated using the relative positions of focus and the recording station. These parameters have been used further in studying the attenuation characteristics.

4.3 ATTENUATION MODEL

Various forms of empirical relations to compute attenuation

TABLE 4.1

Strong Ground Motion Data **

(a) Dharmasala earthquake (April 26, 1986)

(i)	(ii)	(iii)	(iv)	(v)	(vi)
32.12	76.53	83.13	41.57	25.28	142.49
31.98	76.30	36.80	40.27	23.07	57.56
32.03	76.48	19.21	41.92	25.84	36.49
32.20	76.32	94.90	33.15	3.11	182.89
32.13	76.00	15.18	42.72	27.12	16.55
32.08	76.25	95.75	35.13	12.05	144.97
32.10	76.37	94.17	35.41	12.83	145.53
32.20	76.18	147.80	34.29	9.33	243.20
32.30	76.08	33.88	39.78	22.22	50.41

(b) Meghalaya earthquake (September 10, 1986)

(i)	(ii)	(iii)	(iv)	(v)	(vi)
25.97	92.60	20.58	75.29	61.80	44.51
25.18	92.02	37.33	62.23	44.98	88.65
25.35	92.37	18.41	52.39	29.92	45.01
25.68	91.63	48.08	71.02	56.52	90.96
25.90	91.87	21.13	65.30	49.15	54.53
25.50	91.27	10.04	101.49	91.93	19.01
25.65	92.80	21.15	76.24	62.96	47.71
25.30	91.90	26.75	58.91	40.27	90.95
25.72	92.38	58.73	50.65	26.76	135.86
25.50	92.15	26.53	43.67	7.62	111.42
25.50	92.62	11.84	61.76	44.33	31.36
25.73	91.88	28.72	55.74	35.47	99.49

* (i) Latitude (deg.) of epicentre
* (ii) Longitude (deg.) of epicentre
* (iii) Peak horizontal velocity (mm/sec)
* (iv) Hypocentral distance
* (v) Epicentral distance
* (vi) Peak horizontal acceleration (cm/sec/sec)

(c) Burma-India earthquake (May 18, 1987)

(i)	(ii)	(iii)	(iv)	(v)	(vi) **
25.97	92.60	21.56	122.76	112.12	33.59
25.88	93.00	22.00	88.81	73.40	19.42
25.77	93.25	36.20	67.90	45.94	88.46
26.00	93.77	34.28	78.67	60.73	64.40
25.92	93.43	27.69	71.20	50.70	84.33
25.30	93.00	28.56	79.34	61.60	48.40
25.17	93.02	36.93	83.21	66.51	54.42
25.37	93.30	38.07	58.68	30.72	83.86
25.65	93.10	17.71	71.92	51.69	37.04
25.20	93.30	32.35	65.21	41.86	60.07
25.90	91.87	13.12	184.84	177.95	17.08
25.65	92.80	18.11	94.74	80.48	46.43
25.72	92.38	22.84	132.65	122.87	48.53
25.50	92.62	14.50	108.89	96.73	25.02

(d) Tripura-Assam earthquake (February 6, 1988)

(i)	(ii)	(iii)	(iv)	(v)	(vi)
25.40	92.85	20.64	154.59	151.02	23.94
25.97	92.60	13.65	139.53	135.57	29.59
25.88	93.00	10.35	173.92	170.76	16.04
25.18	92.02	18.37	82.61	75.73	37.93
25.30	93.00	29.05	170.46	167.24	36.25
25.17	93.02	19.42	174.74	171.59	33.97
25.65	93.10	9.87	179.40	176.34	24.89
24.82	92.63	10.64	153.46	149.86	9.20
25.35	92.37	47.46	108.59	103.45	78.19
25.45	91.77	43.85	53.62	42.26	79.61
25.68	91.63	52.63	48.10	34.99	112.09
25.90	91.87	26.45	75.83	68.27	84.62
25.30	91.90	21.24	68.09	59.56	48.75
25.72	92.38	32.43	111.38	106.38	64.58
25.55	91.90	16.06	64.56	55.48	46.72
25.50	92.15	22.48	86.81	80.29	55.30
25.50	92.62	31.43	131.36	127.15	45.44
25.73	91.88	36.73	68.02	59.48	59.74

* (i) Latitude (deg.) of epicentre
* (ii) Longitude (deg.) of epicentre
* (iii) Peak horizontal velocity (mm/sec)
* (iv) Hypocentral distance
* (v) Epicentral distance
* (vi) Peak horizontal acceleration (cm/sec/sec)

(e) Gauhati earthquake (August 6, 1988)**

(i)	(ii)	(iii)	(iv)	(v)	(vi)
25.40	92.85	65.68	192.16	169.78	216.82
25.97	92.60	117.05	223.33	204.39	162.06
25.88	93.00	64.03	186.61	163.48	91.50
25.77	93.25	228.19	162.80	135.66	337.07
26.00	93.77	121.36	136.22	102.25	219.78
25.27	91.73	26.78	296.49	282.50	53.65
25.18	92.02	46.87	270.29	254.87	106.60
25.92	93.43	205.55	153.95	124.82	331.37
24.92	92.78	58.89	205.57	184.82	63.05
25.30	93.00	52.05	179.38	155.17	130.21
25.37	93.30	46.43	153.73	124.63	96.27
25.10	92.85	44.39	195.22	173.24	76.68
25.98	92.85	65.61	202.46	181.36	131.05
25.00	92.45	30.40	233.05	214.97	28.91
24.80	93.10	88.30	183.26	159.64	95.71
24.97	92.57	77.76	223.30	204.36	55.80
24.82	92.63	110.74	221.75	202.66	66.55
25.35	92.37	31.74	236.26	218.45	70.10
24.95	93.00	39.04	186.08	162.87	48.24
25.97	91.47	48.61	327.03	314.40	56.78
25.37	91.47	25.18	321.65	308.81	45.33
25.45	91.77	39.17	292.78	278.60	113.14
25.28	91.58	33.67	310.77	297.45	83.63
25.68	91.63	64.50	306.85	293.36	143.47
25.50	91.27	31.04	340.97	328.88	53.23
25.65	92.80	55.19	198.41	176.82	165.44
25.30	91.90	42.13	280.39	265.55	50.37
25.72	92.38	103.63	236.98	219.22	228.28
25.55	91.90	20.44	280.40	265.57	73.50
24.82	92.80	98.76	207.39	186.84	83.38
25.50	92.15	43.95	256.56	240.25	149.76
25.50	92.62	51.66	213.37	193.46	79.04
25.73	91.88	51.94	283.73	269.08	150.16

* (i) Latitude (deg.) of epicentre
* (ii) Longitude (deg.) of epicentre
* (iii) Peak horizontal velocity (mm/sec)
* (iv) Hypocentral distance
* (v) Epicentral distance
* (vi) Peak horizontal acceleration (cm/sec/sec)

of strong motion have been proposed by many workers which have been discussed in Chapter III. These relations should be simple to use in the field by non technical persons, in the absence of detailed subsurface geological information and should not involve too many variables for better estimation of ground motion. For the present study we have used attenuation relation given by Kanai (1961). This relation has been widely used by many workers. Orphal and Lahoud (1974), and Hasegawa et al. (1980) have used Kanai's model to study the attenuation in different geographical regions. Kanai's model which has been used for analysis of magnitude and distance dependence of strong ground motion parameters is simple, and allows a physically meaningful comparison among the attenuation rates of recorded strong motions and intensity data. The empirical formula of Kanai (1961) can be written as,

$$\log_{10} AGM = b_1 + b_2 M - b_3 \log R \qquad (4.1)$$

which can also be expressed as

$$AGM = b_1' \, e^{b_2' M} \, R^{-b_3} \qquad (4.2)$$

where AGM refers to the amplitude of ground motion parameter under consideration, M is earthquake magnitude, R is hypocentral distance, and b_1, b_2, b_3, b_1' and b_2' are coefficients to be determined. These coefficients depends on the geology of the region and can be estimated using accelerograph records and isoseismal maps of the earthquakes.

In order to compare attenuation relations of intensity with those of other AGM parameters, we must make use of empirical relations connecting different parameters of strong ground motion. This has been done in a later section, let us first decide on an

intensity attenuation model which easily permits this comparison. Maximum intensity in the epicentral region is linearly dependent on magnitude. The Modified Mercalli Intensity (I), can be written as (Hasegawa et al. 1980),

$$I = B_1 + B_2 M - B_3 \log R \qquad (4.3)$$

To derive required B_3 attenuation coefficient (equation 4.3), we make use of empirical relations given by Richter (1958)

$$\log a = k_1 I - k_2 \qquad (4.4)$$

$$\log v = k_3 I - k_4 \qquad (4.5)$$

where a and v are peak horizontal ground acceleration and velocity, respectively, and $k_1 - k_4$ are empirical constants. After substituting equation (4.3) into equations (4.4) and (4.5), and comparing with equation (4.1), we get

$$b_3(\text{for } a) = k_1 B_3 \qquad (4.6)$$

and

$$b_3(\text{for } v) = k_3 B_3 \qquad (4.7)$$

Various workers have used either epicentral distance or hypocentral distance in the above equations. This is because of the fact that for low or moderate focal depths the difference in these distances is less and will not effect the resulting equations (Espinosa 1979). Espinosa (1979) has used epicentral distances in his expressions but recognizes that some of the distances used are focal distances.

Individual site intensity data tend to have a very large scatter, so that a range of intensities upto three intensity units can often be observed at same distance from the epicentre.

Consequently, the coefficients in equation (4.3), will have large standard deviations. To provide some initial smoothing of raw intensity data, we have redrawn well-defined isoseismal lines to form a circle with roughly same area as that contained by the original contour. Using any two successive isoseismal lines of intensities I_1 and I_2 at distances R_1 and R_2, equation (4.3) can be written as

$$I_1 = B_1 + B_2M - B_3 \log R_1 ,$$

$$I_2 = B_1 + B_2M - B_3 \log R_2$$

Using above equations, we can write

$$B_3 = \frac{(I_2 - I_1)}{\log (R_1 / R_2)} \qquad (4.8)$$

where R_1 and R_2 are radial distances to successive contours, and I_1 and I_2 are corresponding M.M. Intensities. Estimation of B_3 from the isoseismal maps is discussed in a later section.

Intensity is generally representative of different frequency bands of ground vibration. The intensity data have been used to estimate attenuation coefficients of strong ground motion. The dominant ground vibration frequencies will decrease with increasing distance because of the more rapid attenuation of higher frequency waves. These factors suggest that intensity provides, at best, only a gross measure of strong ground motion attenuation. We have used intensity data to place rough limits on only distance attenuation coefficient b_3, and will employ these data for calculating peak horizontal acceleration (PHA) and peak horizontal velocity (PHV) using equations (4.6) and (4.7).

4.4 ISOSEISMAL MAPS

An average B_3 value for northern India has been derived from the observations of intensity attenuation (equation 4.8) using isoseismal data of past earthquakes.

Earthquake isoseismal maps provide valuable documents of macro-seismic effects of large earthquakes. These maps are the products of direct field observations immediately following earthquake occurrences. Isoseismal maps of past earthquakes help us to understand nature of the earthquakes in a particular region. Isoseismal maps of major earthquakes of India have been used in the present study. The data obtained from these isoseismal maps are used for estimating B_3 value and to study the intensity attenuation. The isoseismal maps used for this study are of Assam earthquake (July 1897), Kangra earthquake (April 1905), Calcutta earthquake (September 1906), Bangladesh earthquake (July 1918), Dhubri earthquake (July 1930), Bihar-Nepal earthquake (January 1934), Anjar earthquake (July 1956), Koyana Earthquakes (September 1967, December 1967, August 1968), Gauhati earthquake (July 1975), and Dharmasala earthquake (April 1986). Isoseismal maps of these earthquakes are shown in Figures 4.1 to 4.10. Brief description of these earthquakes and their effects, based on isoseismal maps, are given below:

Assam earthquake (1897):

Assam earthquake (Figure 4.1) having magnitude of 8.7 and epicentral intensity of XII on M.M. scale, occurred in Shillong in Assam on June 12, 1897 is the biggest earthquake of India. Oldham (1926) estimated focal depth as around 100-200 miles. The shock was felt over a wide area of 4,550,000 sq. km.

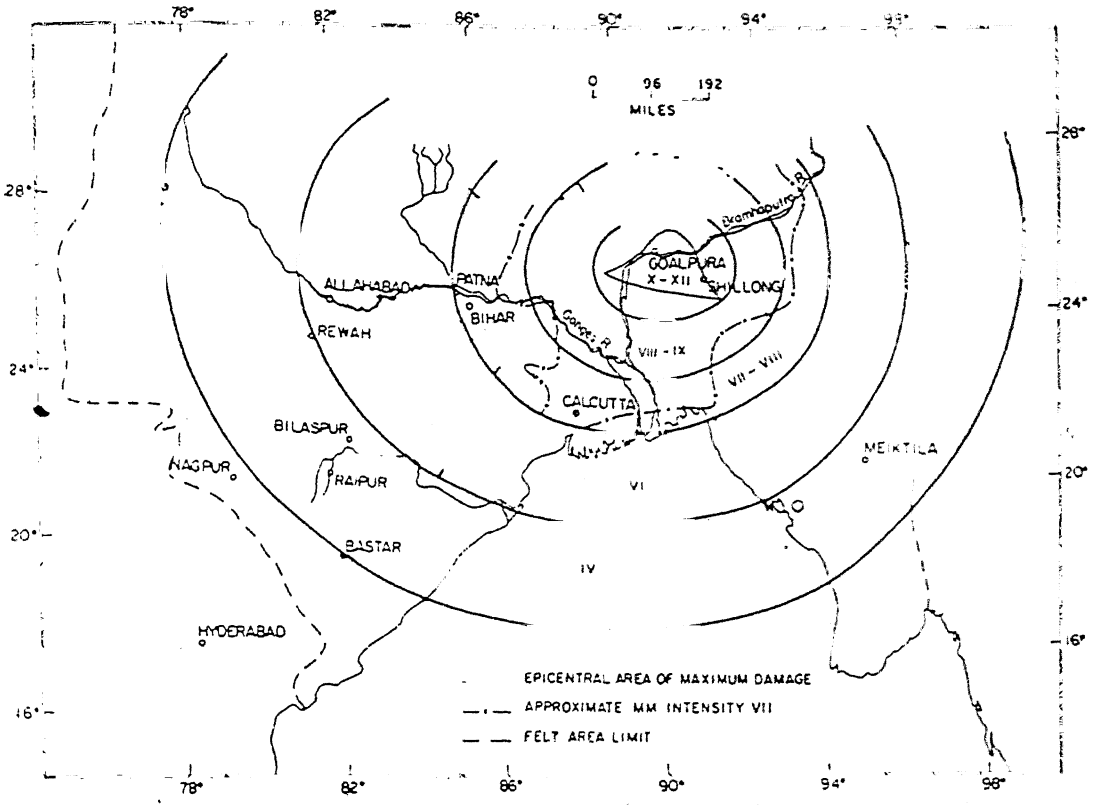

Fig. 4.1 Isoseismal map of Assam earthquake (July 1897)

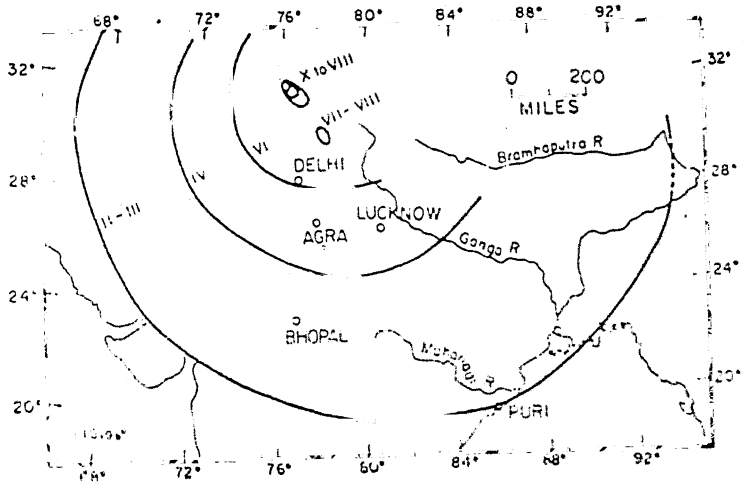

Fig. 4.2 Isoseismal map of Kangra earthquake (April 1905)

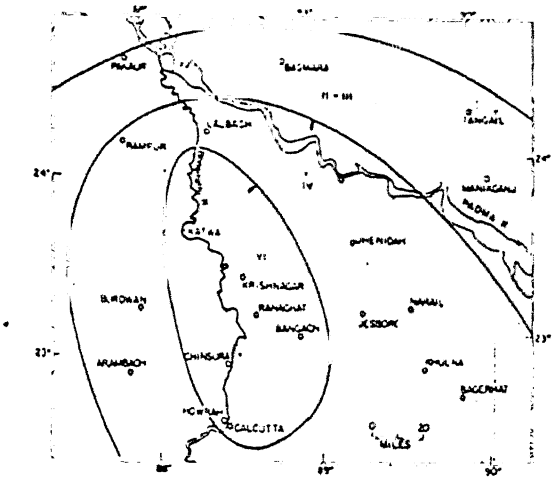

Fig. 4.3 Isoseismal map of Calcutta earthquake (September 1906)

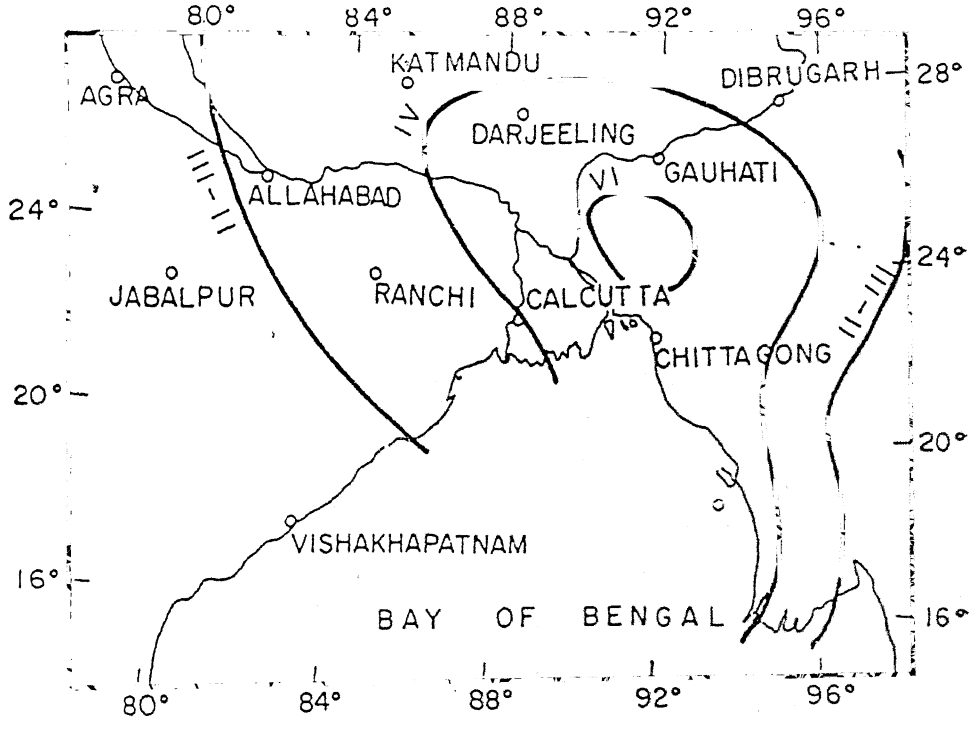

Fig. 4.4 Isoseismal map of Bangladesh earthquake (July 1918)

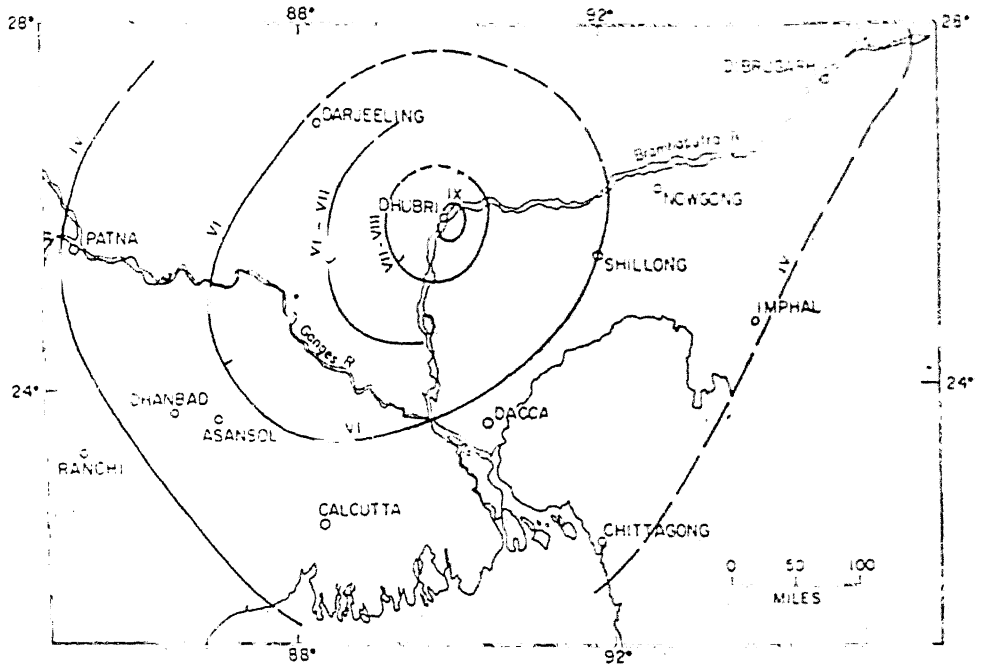

Fig. 4.5 Isoseismal map of Dhubri earthquake (July 1930)

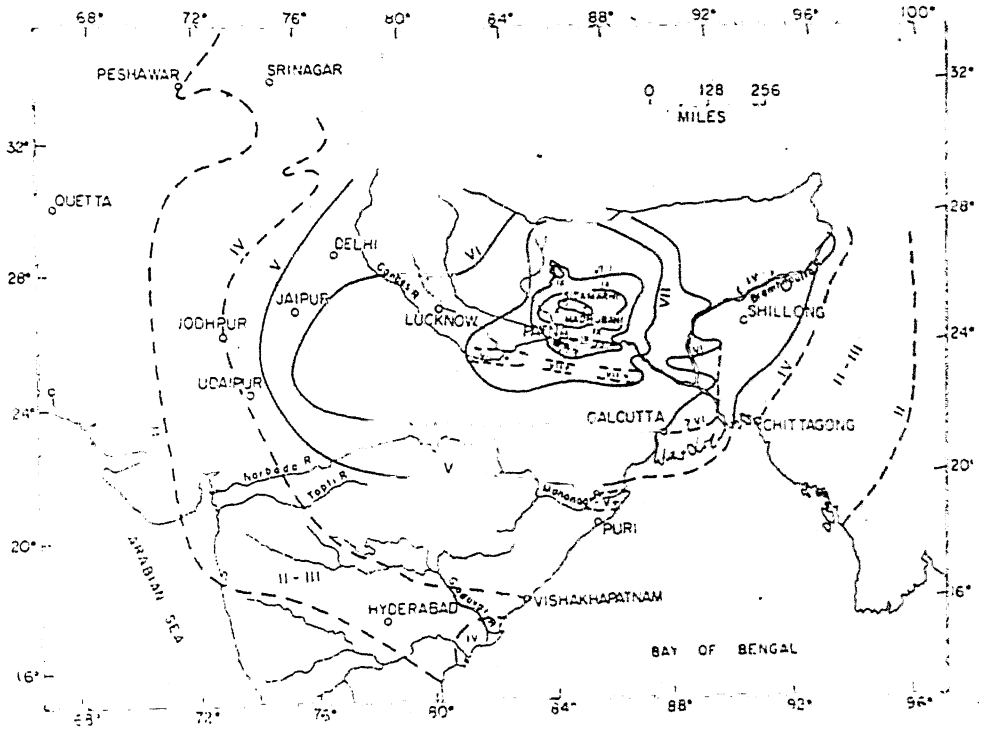

Fig. 4.6 Isoseismal map of Bihar-Nepal earthquake (January 1934)

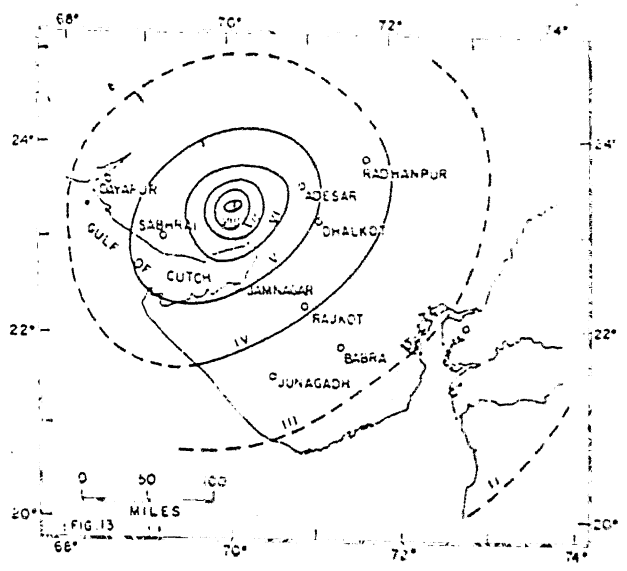

Fig. 4.7 Isoseismal map of Anjar earthquake (July 1956)

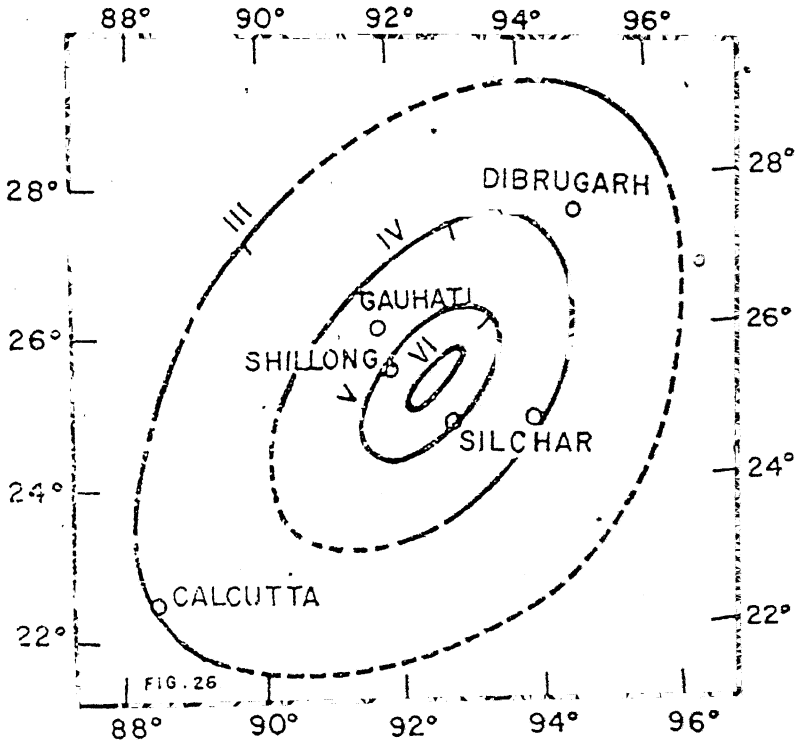

Fig. 4.9 Isoseismal map of Gauhati earthquake (July 1975)

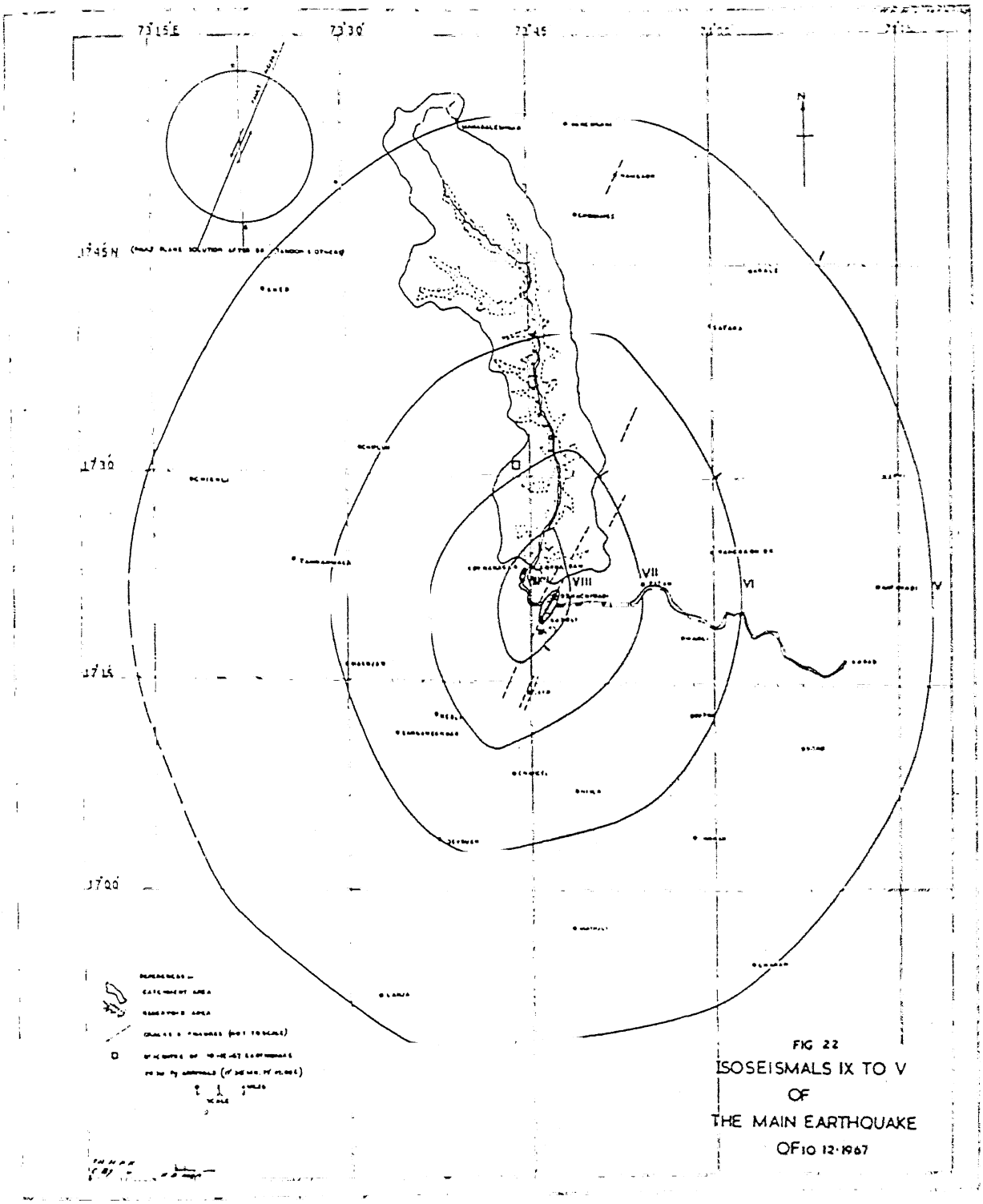

Fig. 4.8 Isoseismal map of Koyana earthquake (December 1967)

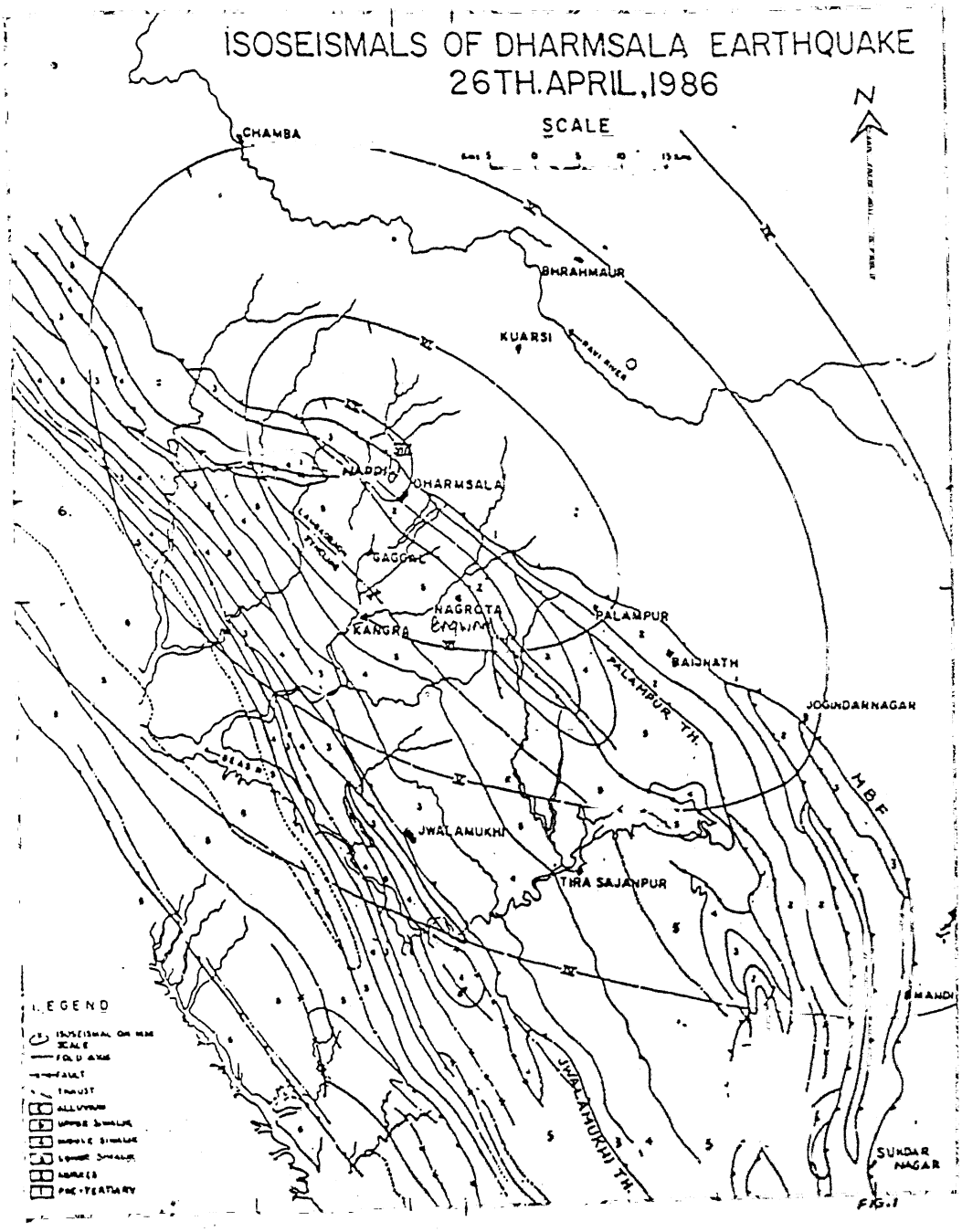

Fig. 4.10 Isoseismal map of Dharmasala earthquake (April 1986)

Kangra earthquake (1905):

The Kangra earthquake (Figure 4.2) of magnitude 8.6 occurred in Himachal Pradesh on April 4, 1905 with epicentral intensity X on M.M. scale. Middlemiss (1910) determined the depth of focus between 21 to 40 miles. The shock was felt over an area of 1,625,000 sq. miles.

Calcutta earthquake (1906):

Middlemiss (1907) has studied this earthquake (Figure 4.3). He reported that people living in an area of 50,000 sq. miles have felt this earthquake. No estimate of magnitude is available. The earthquake occurred on September 29, 1906 with an epicentral intensity of VI on M.M. scale.

Bangladesh earthquake (1918):

Sirimangal experienced an earthquake of magnitude 7.6 on July 8, 1918. The isoseismal map (Figure 4.4) is given by Sturt (1920). The maximum intensity reached was X on M.M. scale at the epicentral area. The depth of focus as calculated by Stuart (1920) is around 8-9 miles. This earthquake has been felt over an area of 800,000 sq. miles.

Dhubri earthquake (1930):

Dhubri earthquake occurred on July 3, 1930 with an epicentral intensity of IX on M.M. scale and magnitude of 7.1 (Figure 4.5). This earthquake felt over an area of 322,000 sq. miles (Gee 1934).

Bihar-Nepal earthquake (1934):

In the Himalayan foothills a major earthquake of magnitude 8.4 occurred near Bihar-Nepal border, on January 15, 1934 (Figure 4.6). Maximum intensity of X on M.M. scale has been observed. The earthquake damage has been surveyed by Geological Survey of India

(1939). The high intensity region of the Nepal valley has been attributed to the presence of unconsolidated alluvium. Earthquake damage has largely been found along river banks and in low lying water-logged areas bordering the rivers. It has found to be less on thick clay beds. Damage has also been intense on unstable hill slopes. The elliptical shape of the isoseismal lines is due to the subsurface structure (G.S.I. 1939). The shock has been felt over an area of 4,920,000 sq. km, and depth of focus has been around 14.8 km (Roy 1939). However, Richter (1958) estimated focus around a depth of 20-30 km.

Anjar (Kutch) earthquake (1956):

In Kutch region an earthquake of magnitude 7.0 has been occurred on July 21, 1956 near Anjar town. The maximum intensity very nearly reached IX at few places (Figure 4.7). The radius of perceptibility of this shock has been reported to be 330 km. and depth of focus has been estimated between 13 to 18 km. Tandon (1959) observed severe damage in eastern portion of the Anjar town than those to the western part. He attributed this tc the fact that the eastern part of the town has been built on soft ground whereas western part is situated on hard trap rocks.

Koyana Earthquake (1967):

Koyana earthquake in the peninsular shield of December 10, 1967 with magnitude 7.0 has been found to be most destructive. The isoseismal map given by Central Water and Power Research Station (CWPRS), India has been reproduced in Figure 4.8. The maximum intensity of this earthquake almost reached the value IX. The earthquake has been felt over an area of 697,600 sq.km. (Mukherjee 1971).

Assam earthquake (1975):

Gosavi et al. (1977) studied Assam earthquake of July 8, 1975. The earthquake with magnitude 6.7 and focal depth 60 km. has been felt over an area of 800 km. radius. The intensity reached the value VII on M.M. scale at the epicentre (Figure 4.9), which was close to that of the 1897 earthquake, indicating activity along the same neighbouring thrust zone.

Dharmasala earthquake (1986):

Dharmasala earthquake of April 26, 1986 with magnitude of 5.7 and epicentral intensity of VIII on M.M. scale, occurred in Himachal Pradesh. The isoseismal map has been shown in Figure 4.10.

4.4.1 ESTIMATION OF B_3

To estimate B_3 using equation (4.8), we have adopted the following procedure. The area bounded by each isoseismal line is calculated using Planimeter. The area of an isoseism increases with decrease in the intensity. Using this area, we have calculated radius of corresponding circular isoseism assuming subsurface structure as homogeneous media. This assumption has less effect on attenuation relationship of strong ground motion (equation 4.1), as we are using intensity data to place rough limits on only distance attenuation coefficient b_3. Table 4.2 shows the calculated isoseismal areas and corresponding radii for different earthquakes. Using these data, we have calculated B_3 value for each pair of isoseisms using equation 4.8 (Table 4.2). The range of B_3 values and hypocentral distances for different earthquakes have been given in Table 4.2. The average value of B_3

TABLE 4.2

Estimation of B_3

I_1	I_2	A_1	A_2	R_1	R_2	B_3
		sq.miles	sq.miles	km.	km.	
6	7	675869.6	278709.1	746.4	479.3	5.23
7	8	278709.1	125419.0	479.3	321.5	5.70
8	9	3705.0	1416.6	55.2	34.2	4.79
4	6	29431.0	4484.1	155.8	60.8	4.89
6	7	15995.7	7020.3	114.8	76.1	5.59
6	6.5	65080.5	34596.7	231.6	168.9	3.65
7	8	34596.7	5322.6	168.9	66.2	2.46
6	7	322303.1	109094.5	515.5	299.9	4.25
6	8	322303.1	33202.7	515.5	165.4	4.05
6	9	322303.1	11858.1	515.5	98.9	4.18
6	10	322303.1	1660.1	515.5	37.0	3.49
7	8	109094.5	33202.7	299.9	165.4	3.87
7	9	109094.5	11858.1	299.9	98.9	4.15
7	10	109094.5	1660.1	299.9	37.0	3.30
8	9	33202.7	11858.1	165.4	98.9	4.47
8	10	33202.7	1660.1	165.4	37.0	3.07
9	10	11858.1	1660.1	98.9	37.0	2.35
4	5	38829.1	17323.7	178.9	119.5	5.69
3	4	112665.1	45965.8	304.7	194.7	5.14
4	5	45965.8	14474.3	194.7	109.2	3.98
5	6	14474.3	4694.4	109.2	62.2	4.09
6	7	4694.4	1564.8	62.2	35.9	4.19
7	8	1564.8	586.7	35.9	22.0	4.69
5	6	249.5	28.6	14.3	4.9	2.13
5	6	4093.3	1191.6	58.1	31.3	3.73
6	7	1191.6	330.1	31.3	16.5	3.53
7	8	330.1	42.8	16.5	5.9	2.26
6	7	765.3	233.2	25.1	13.8	2.13
7	8	233.2	40.7	13.8	5.8	2.64
4	5	356.8	67.2	17.2	7.5	2.75
3	4	252525.4	73972.1	456.2	246.9	3.75
3	5	252525.4	15304.6	456.2	112.3	3.28
4	5	73972.1	15304.6	246.9	112.3	2.92
5	6	1689.5	403.9	37.3	18.2	3.22
6	7	403.9	28.7	18.2	4.8	1.74
5	7	1689.5	28.7	37.3	4.8	2.26

= 3.9713 has been found for northern India.

4.5 ATTENUATION RELATION FOR PEAK HORIZONTAL ACCELERATION

Using AGM relation given in equation (4.2), peak horizontal acceleration (PHA) is written as

$$a = b_1' e^{b_2' M} R^{-b_3} \qquad (4.9)$$

This equation has three variables a, M and R, and three coefficients b_1', b_2' and b_3 which have to be determined. These coefficients vary from region to region. For Indian region so far no estimates of these coefficients have been made. The value of b_3 can be obtained using equation (4.6) as

$$b_3(\text{for } a) = k_1 B_3$$

The value k_1=0.35 has been adopted based on 1300 world wide observations (Murphy and O'Brien 1977). The average computed value of B_3 for northern India is 3.9713. Substituting B_3 and k_1 values in equation (4.6), we get

$$b_3 \text{ (for a)} = 0.35 \times 3.9713$$
$$= 1.39$$

Now substituting b_3 value in equation (4.9), we get

$$a = b_1' e^{b_2' M} R^{-1.39}$$

where a = PHA in (cm sec^{-2})
R = hypocentral distance (km.)

M = magnitude.

Performing a regression analysis on the data given in Table 4.1, and using above equation, we get,

$$b_1' = 4.55103 \text{ and } b_2' = 1.47385$$

The relation for attenuation of peak horizontal ground acceleration for Northern India is written as

$$a \text{ (cm sec}^{-2}) = 4.55103\ e^{1.47385M_R - 1.39} \qquad (4.10)$$

Equation (4.10) is an empirical relation which has been given based on the strong ground motion data as well as the data obtained from the analysis of isoseismal maps of Indian earthquakes. We have fit the data of each earthquake in the form of equation (4.9) and the following equations for different earthquakes have been obtained:

Dharmasala earthquake (April 26, 1986):

$$a \text{ (cm sec}^{-2}) = 3.503 \times 10^{13}\ R^{-7.347}\ g \qquad (4.11)$$

Meghalaya-Assam earthquake (September 10, 1986):

$$a \text{ (cm sec}^{-2}) = 158.33 \times R^{-1.897}\ g \qquad (4.12)$$

Burma-India earthquake (May 18, 1987):

$$a \text{ (cm sec}^{-2}) = 10.3092 \times R^{-1.206}\ g \qquad (4.13)$$

Tripura-Assam earthquake (February 6, 1988):

$$a \text{ (cm sec}^{-2}) = 5.533 \times R^{-1.047}\ g \qquad (4.14)$$

Gauhati earthquake (August 6, 1988):

$$a \text{ (cm sec}^{-2}) = 45.7985 \times R^{-1.13}\ g \qquad (4.15)$$

and for the combined data of all earthquakes having M=5.7, we have obtained following equation

$$a\ (\text{cm sec}^{-2}) = 4.623 \times R^{-1.044}\ g \qquad (4.16)$$

We have plotted variation of horizontal acceleration with distance for different earthquakes using equations (4.11) to (4.16) in Figures 4.11-4.16. The superimposed points are observed accelerations at different recording stations. It has been found that the peak horizontal acceleration decreases with increasing hypocentral distance. The slope of the plot of Dharmasala earthquake is very high compared to the slopes of other lines. This may be due to the fact that the presence of hard and rocky soil in Dharmasala region (H.P). Using equation (4.10), we have studied the variation of peak horizontal acceleration with earthquake magnitude for northern India (Figure 4.17). It is observed that peak horizontal acceleration increases with increasing earthquake magnitude and decreases with increasing hypocentral distance. Figure 4.18 shows the variation of peak horizontal acceleration with hypocentral distance for different magnitudes, for northern India.

4.5.1 COMPARATIVE STUDY OF ACCELERATION ATTENUATION

We have made an effort to compare peak acceleration relation (equation 4.10) for India with the similar relations exist for other parts of the world. Hasegawa et al. (1980) have given peak horizontal acceleration relation for western Canada as

$$a\ (\text{cm sec}^{-2}) = 10\ e^{1.3M}\ R^{-1.5}$$

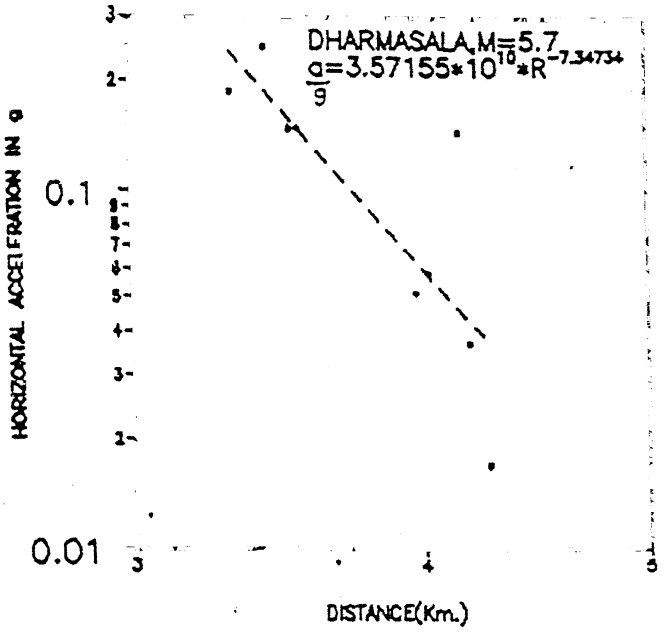

Fig. 4.11 Variation of peak horizontal acceleration with distance for Dharmasala earthquake

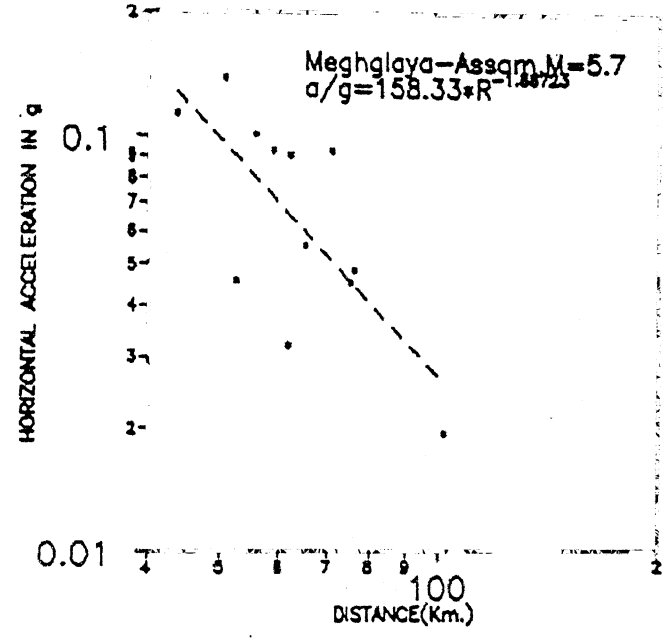

Fig. 4.12 Variation of peak horizontal acceleration with distance for Meghalaya earthquake

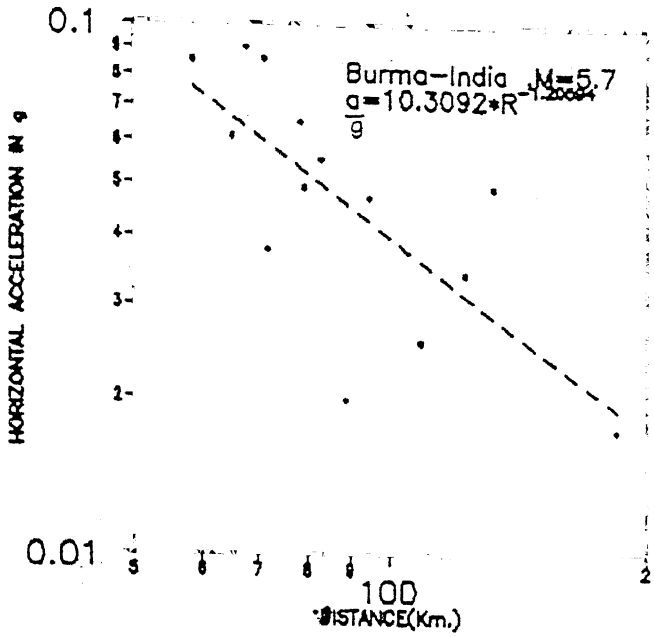

Fig. 4.13 Variation of peak horizontal acceleration with distance for Burma-India earthquake

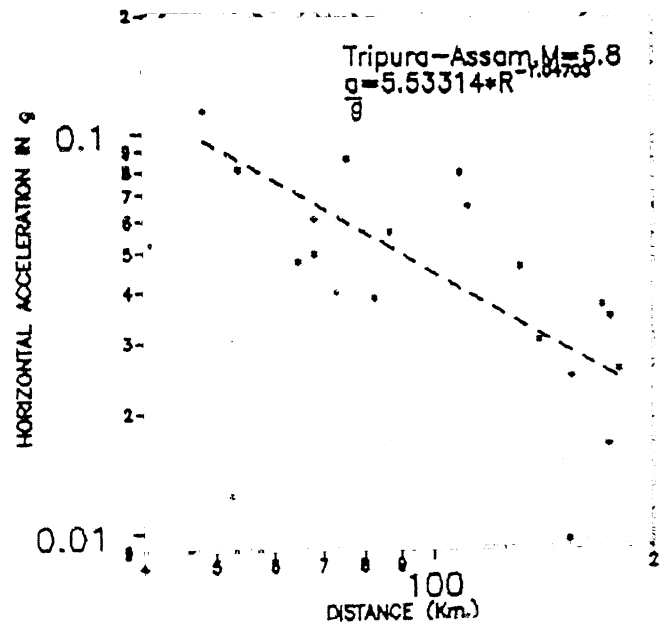

Fig. 4.14 Variation of peak horizontal acceleration with distance for Tripura-Assam earthquake

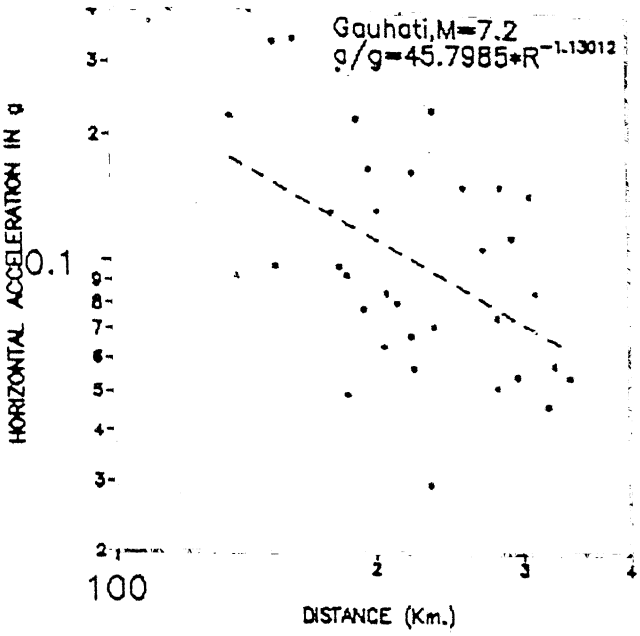

Fig. 4.15 Variation of peak horizontal acceleration with distance for Gauhati earthquake

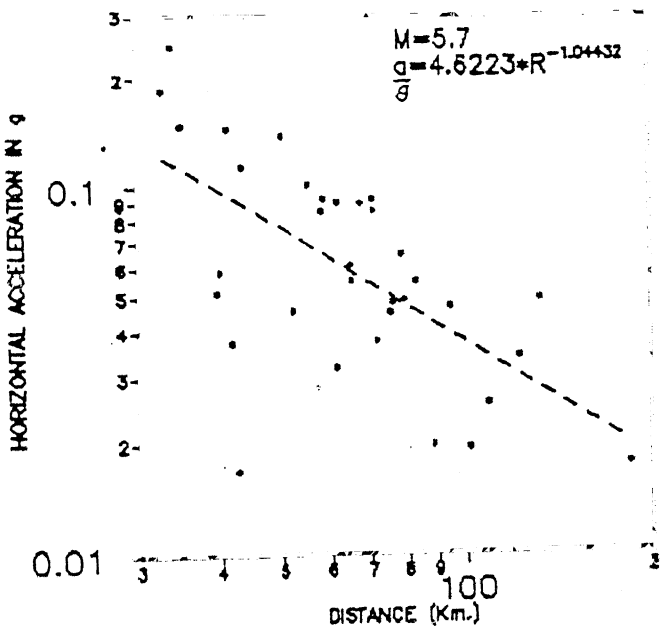

Fig. 4.16 Variation of peak horizontal acceleration with distance for magnitude, M = 5.7

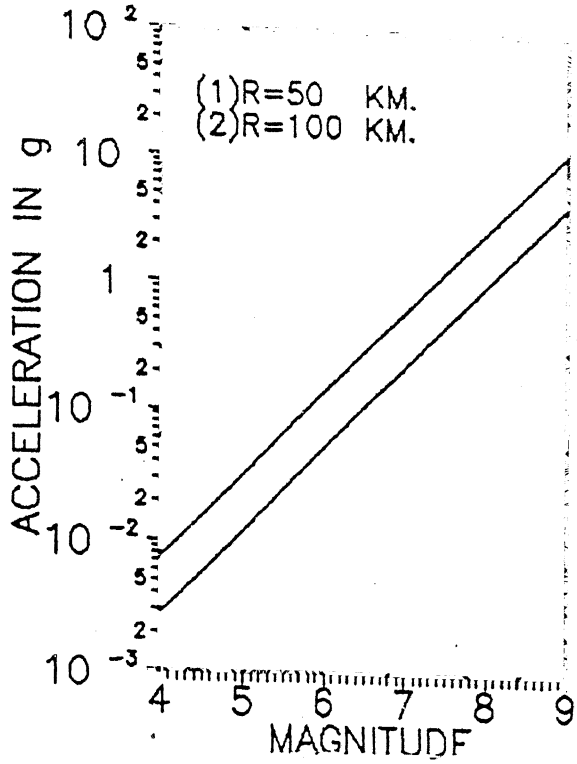

Fig. 4.17 Variation of peak horizontal acceleration with magnitude for northern India

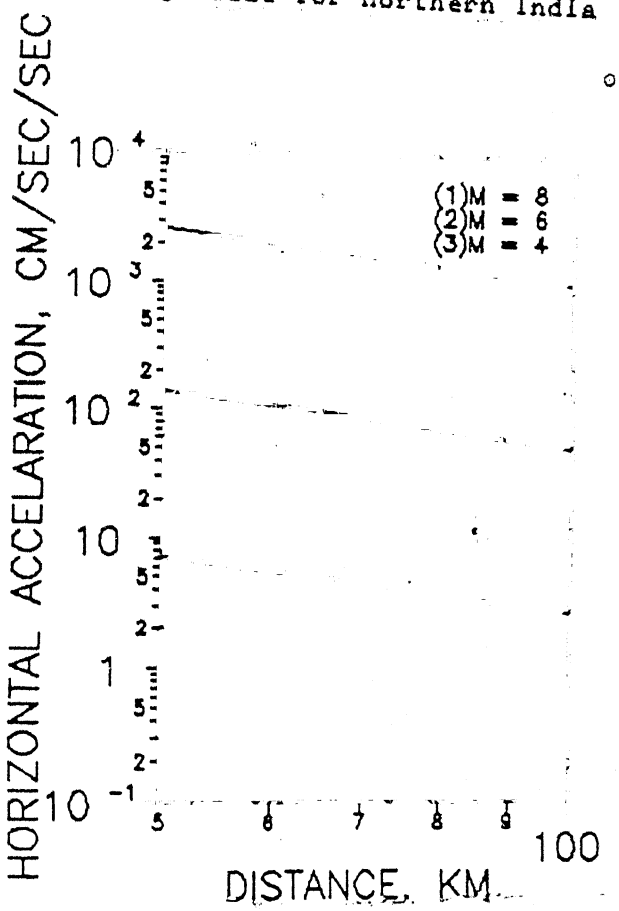

Fig. 4.18 Variation of peak horizontal acceleration with hypocentral distance for northern India

and for eastern Canada,

$$a\ (cm\ sec^{-2}) = 3.4\ e^{1.3M}\ R^{-1.1}$$

In Figure 4.19, we have shown the variation of PHA with hypocentral distance for North India, Eastern Canada and Western Canada for a fixed magnitude M=8.0. It has been found that the PHA values are higher in case of Northern India to those of Canada. For lower magnitude of M=4.0, peak horizontal values are found higher for Canada to those of northern India (Figure 4.20). From this observation it is concluded that higher magnitude earthquakes in India produce comparatively higher peak horizontal values.

4.6 ATTENUATION RELATION FOR PEAK HORIZONTAL VELOCITY

Replacing AGM (Amplitude of Ground Motion) in equation (4.1) by peak horizontal velocity (v), we obtain

$$\log v = b_1 + b_2 M - b_3 \log R \qquad (4.17)$$

In this equation v, M and R are variables and b_1, b_2 and b_3 are coefficients which are to be determined. Using equation (4.7),

$$b_3\ (\text{for } v) = k_3 B_3$$

The value of k_3 = 0.29 is adopted for peak velocity (Espinosa 1977). Substituting the values of B_3 and k_3 in equation (4.7)

$$b_3\ (\text{for } v) = 0.29 \times 3.9713$$
$$= 1.2$$

The coefficient b_2 is fixed based on theoretical considerations. Kanamori and Jennings (1978) have proved that log v is

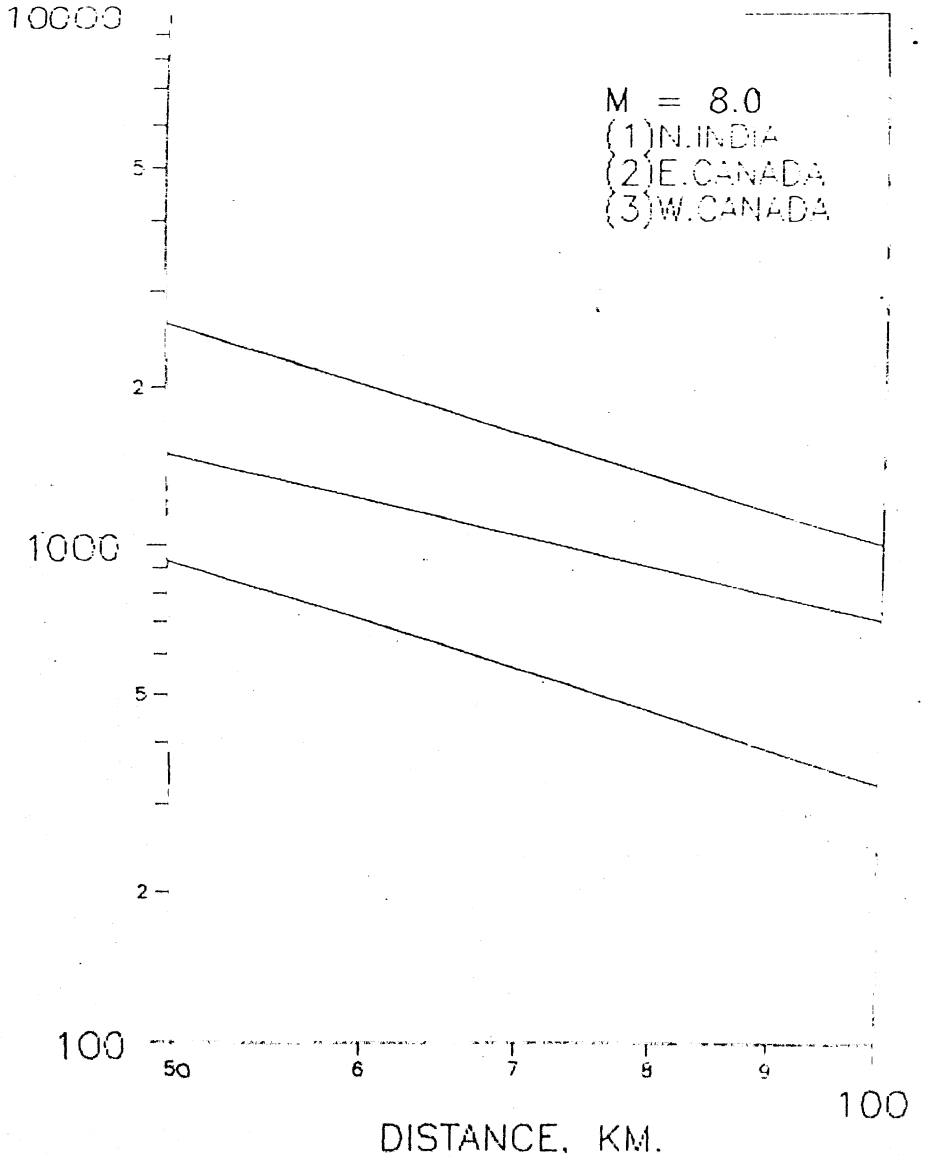

Fig. 4.19 Sample comparison of acceleration-distance correlations for various geographical regions using the three variable covariance relations for M = 8.0

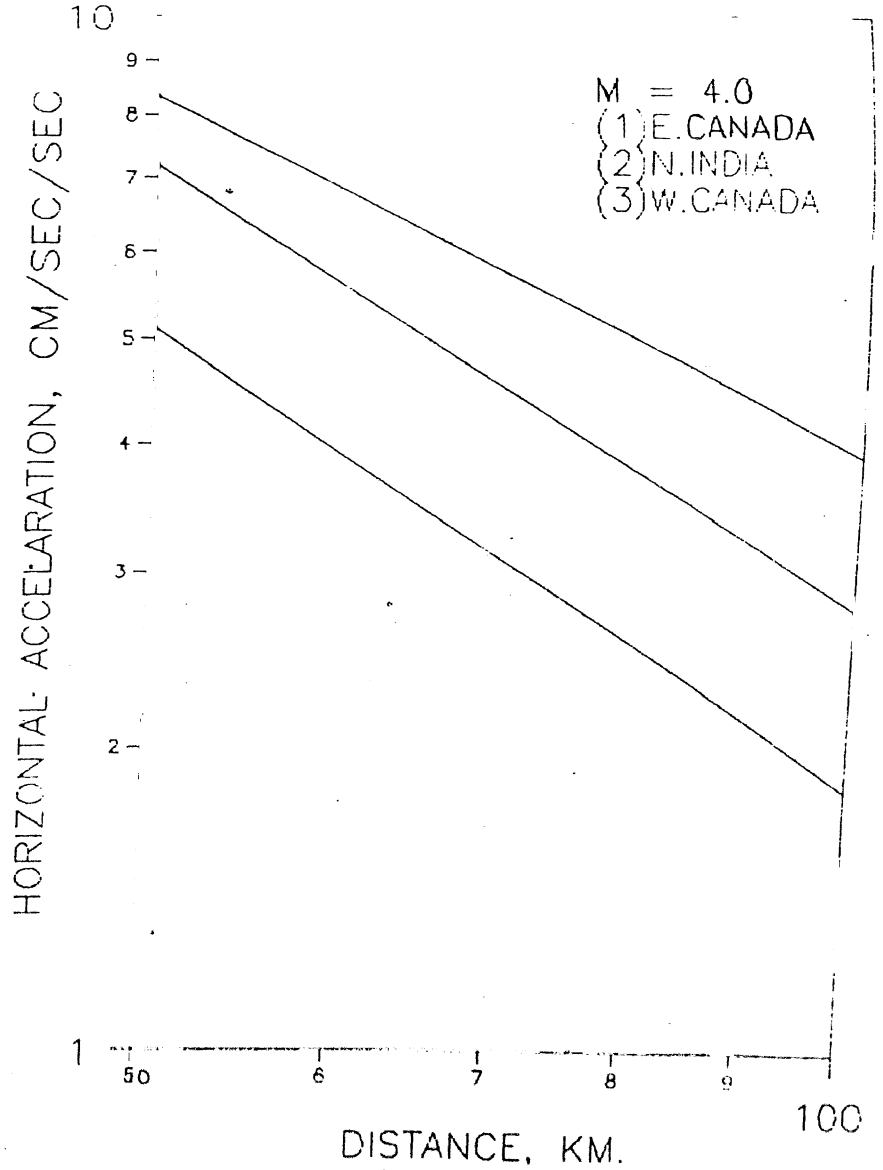

Fig. 4.20 Sample comparison of acceleration-distance correlations for various geographical regions using the three variable covariance relations for M = 4.0

proportional to magnitude, i.e., $b_2 = 1.0$. Nuttli and Herrmann (1978) have also suggested $b_2 = 1.0$ on the basis of theoretical considerations.

Substituting $b_2=1.0$ and $b_3=1.2$ in equation (4.16), we get

$$\log v = b_1 + M - 1.2 \log R$$

or

$$v R^{1.2} = b_1' e^{2.3M} \qquad (4.18)$$

Performing regression analysis on the data given in Table 4.1 using equation (4.18), we obtain

$$b_1' = 0.0027303 \text{ (for v in mm/sec)}$$

The relation for attenuation of peak horizontal velocity is now given as

$$v \text{ (mm sec}^{-1}) = 0.0027303\, e^{2.3M}\, R^{-1.2} \qquad (4.19)$$

where R is the hypocentral distance (km), M is the magnitude and v is the peak horizontal velocity (mm/sec).

Figure 4.21 shows distance attenuation of velocity for different magnitude values for northern India. It has been observed that peak horizontal velocity decreases with increasing distance. Using the data given in Table 4.1 we have obtained the following relations for peak velocity for different earthquakes.

Dharmasala earthquake (April 26, 1986):

$$v \text{ (mm sec}^{-1}) = 2.360 \times 10^{12}\, R^{-6.732} \qquad (4.20)$$

Meghalaya-Assam earthquake (September 10, 1986):

$$v \text{ (mm sec}^{-1}) = 2160.5 \times R^{-1.083} \qquad (4.21)$$

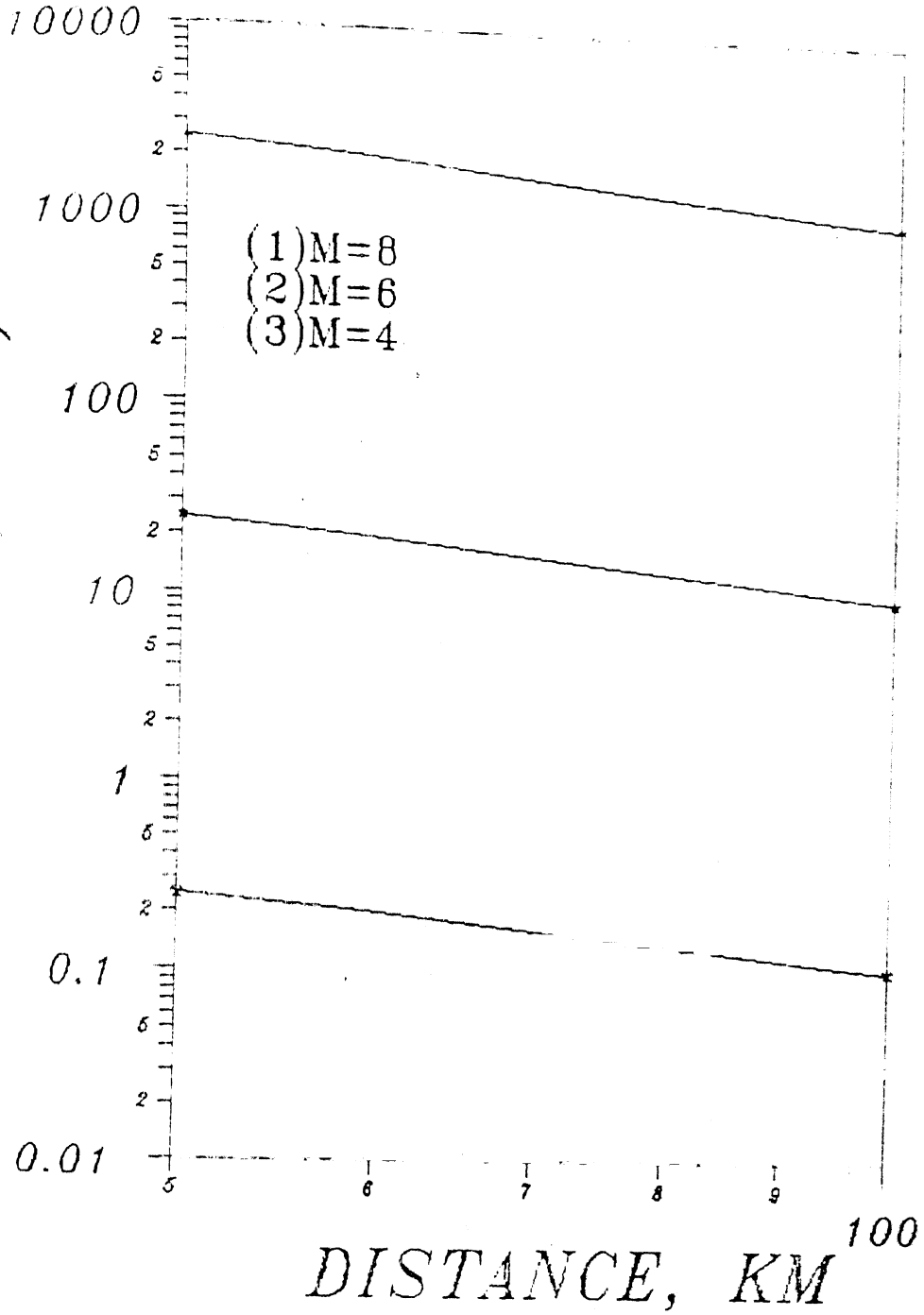

Fig. 4.21 Variation of velocity with distance for northern India

Burma-India earthquake (May 18, 1987):

$$v\ (\text{mm sec}^{-1}) = 953.403 \times R^{-0.815} \qquad (4.22)$$

Tripura-Assam earthquake (February 6, 1988):

$$v\ (\text{mm sec}^{-1}) = 528.7 \times R^{-0.677} \qquad (4.23)$$

Gauhati earthquake (August 6, 1988):

$$v\ (\text{mm sec}^{-1}) = 154427.0 \times R^{-1.13} \qquad (4.24)$$

and for the combined data of all the earthquakes having M=5.7, we have found

$$v\ (\text{mm sec}^{-1}) = 1806.84\ R^{-0.9873} \qquad (4.25)$$

Using equations (4.20) to (4.25) we have plotted the variation of peak horizontal velocity with distance for different earthquakes (Figures 4.22 - 4.27). The superimposed points on these plots are different data points. It has been found that peak horizontal velocity attenuates more rapidly for Dharmasala earthquake than that of the other earthquakes.

4.6.1 COMPARATIVE STUDY OF VELOCITY ATTENUATION

Hasegawa et al. (1980) have given the following attenuation relation for western Canada

$$v = 0.004\ e^{2.3M}\ R^{-1.3} \qquad (4.26)$$

and for eastern Canada

$$v = 0.0018\ e^{2.3M}\ R^{-1.0} \qquad (4.27)$$

where v is peak horizontal velocity (mm/sec) and R is the

Burma-India earthquake (May 18, 1987):

$$v\ (\text{mm sec}^{-1}) = 953.403 \times R^{-0.815} \quad (4.22)$$

Tripura-Assam earthquake (February 6, 1988):

$$v\ (\text{mm sec}^{-1}) = 528.7 \times R^{-0.677} \quad (4.23)$$

Gauhati earthquake (August 6, 1988):

$$v\ (\text{mm sec}^{-1}) = 154427.0 \times R^{-1.13} \quad (4.24)$$

and for the combined data of all the earthquakes having M=5.7, we have found

$$v\ (\text{mm sec}^{-1}) = 1806.84\ R^{-0.9873} \quad (4.25)$$

Using equations (4.20) to (4.25) we have plotted the variation of peak horizontal velocity with distance for different earthquakes (Figures 4.22 - 4.27). The superimposed points on these plots are different data points. It has been found that peak horizontal velocity attenuates more rapidly for Dharmasala earthquake than that of the other earthqakes.

4.6.1 COMPARATIVE STUDY OF VELOCITY ATTENUATION

Hasegawa et al. (1980) have given the following attenuation relation for western Canada

$$v = 0.004\ e^{2.3M}\ R^{-1.3} \quad (4.26)$$

and for eastern Canada

$$v = 0.0018\ e^{2.3M}\ R^{-1.0} \quad (4.27)$$

where v is peak horizontal velocity (mm/sec) and R is the

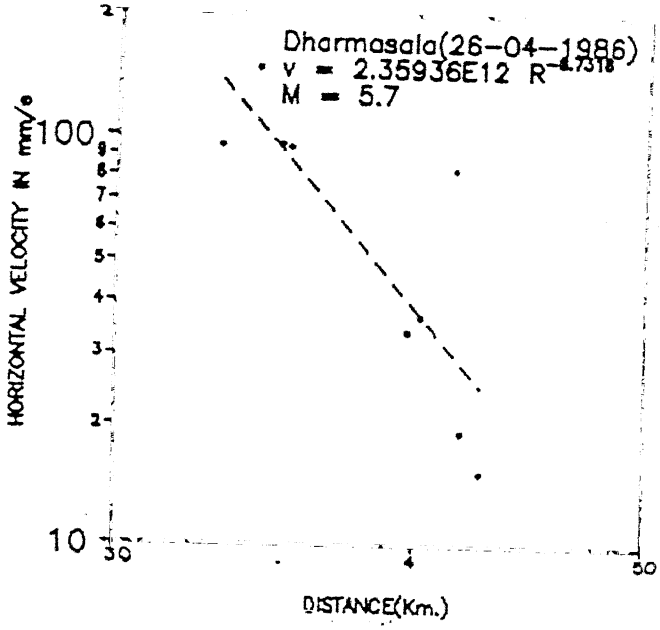

Fig. 4.22 Variation of velocity with distance for Dharmasala earthquake

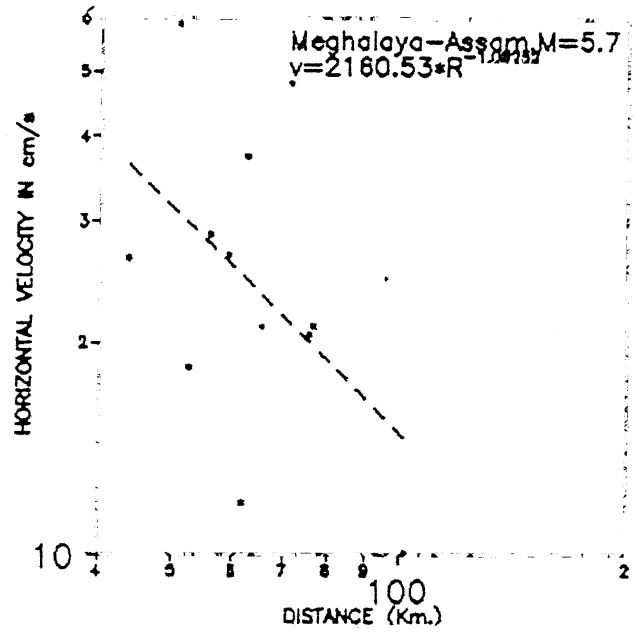

Fig. 4.23 Variation of velocity with distance for Meghalaya earthquake

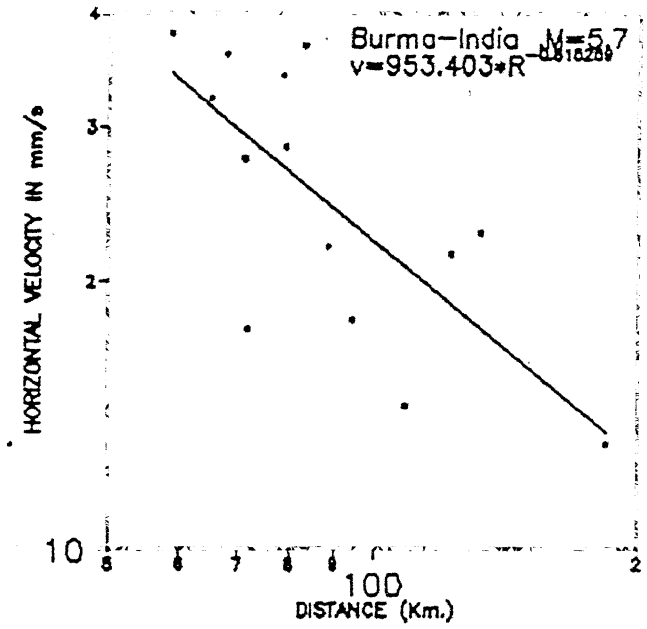

Fig. 4.24 Variation of velocity with distance for Burma-India earthquake

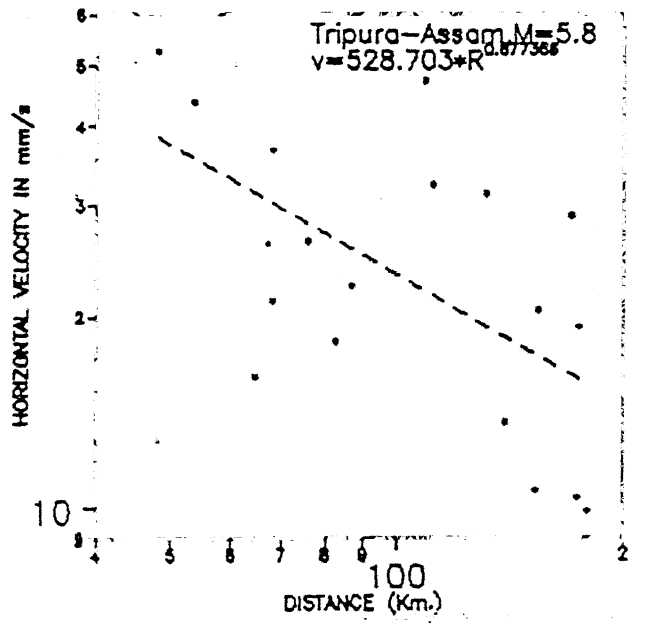

Fig. 4.25 Variation of velocity with distance for Tripura-Assam earthquake

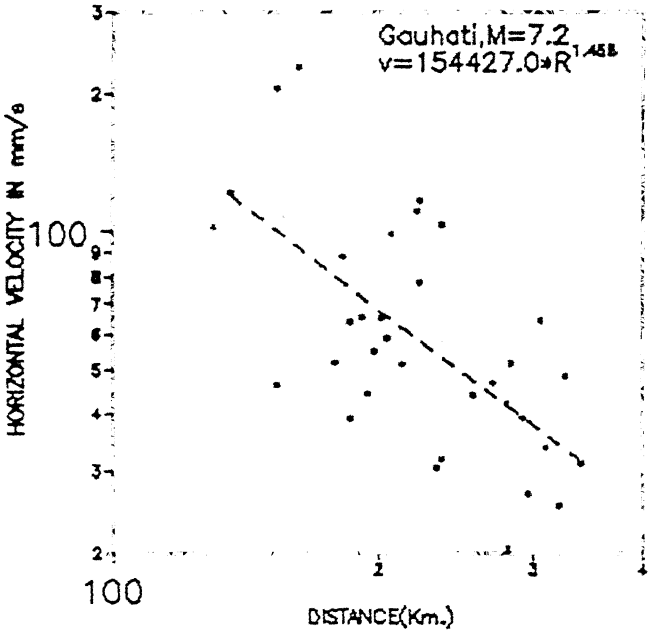

Fig. 4.26 Variation of velocity with distance for Gauhati earthquake

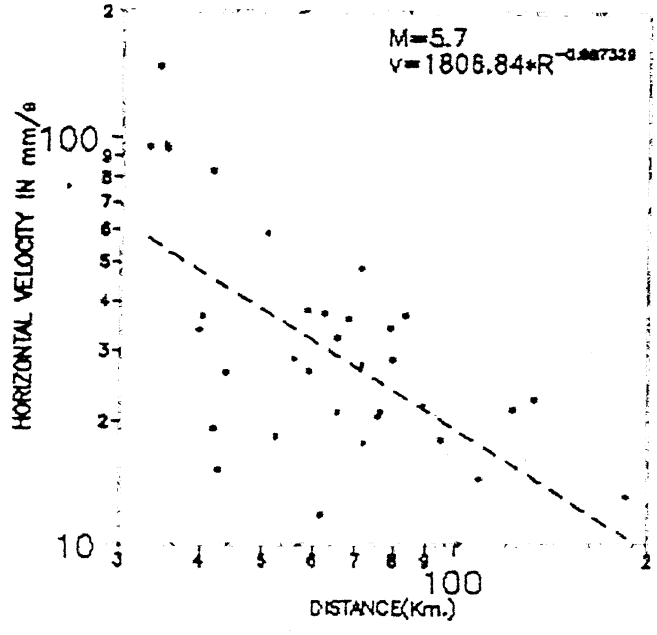

Fig. 4.27 Variation of velocity with distance for magnitude, m = 5.7

hypocentral distance (km).

Figure 4.29 shows the variation of peak horizontal velocity with distance for different geographical regions. It has been found that the attenuation of peak velocity is similar for northern India and western Canada.

4.7 INTENSITY-DISTANCE RELATIONS FOR MAJOR INDIAN EARTHQUAKES

Earthquake Intensity shows level of destruction in the area after an earthquake. Intensity is measured from the damages, surface manifestations and feelings by the people living in the region, immediately after the earthquake. Generally, Intensity is maximum at the epicentre and decreases with the distance from the epicentre i.e., epicentral distance (Δ). We have derived Intensity-distance relations using epicentral distances as given in Table 4.2.

We have plotted Intensity-distance data (Table 4.2) obtained from isoseismal lines, for each earthquake. It has been found that in most of the cases the data points are fitted by straight lines. The slope (s), of these lines indicate decay rate of intensity with epicentral distance. While plotting these graphs we have adopted an additional data point in each graph, at $\Delta=0$, $I=I_0$, which is not given in Table 4.2. From these plots (Figures 4.30 - 4.35) the Intensity-distance pattern follows a relation,

$$\log I = \log I_0 - s\,\Delta \qquad (4.28)$$

This equation can be written as,

$$\frac{I}{I_0} = 10^{-s\Delta} = e^{-2.3s\Delta} = e^{-k\Delta} \qquad (4.29)$$

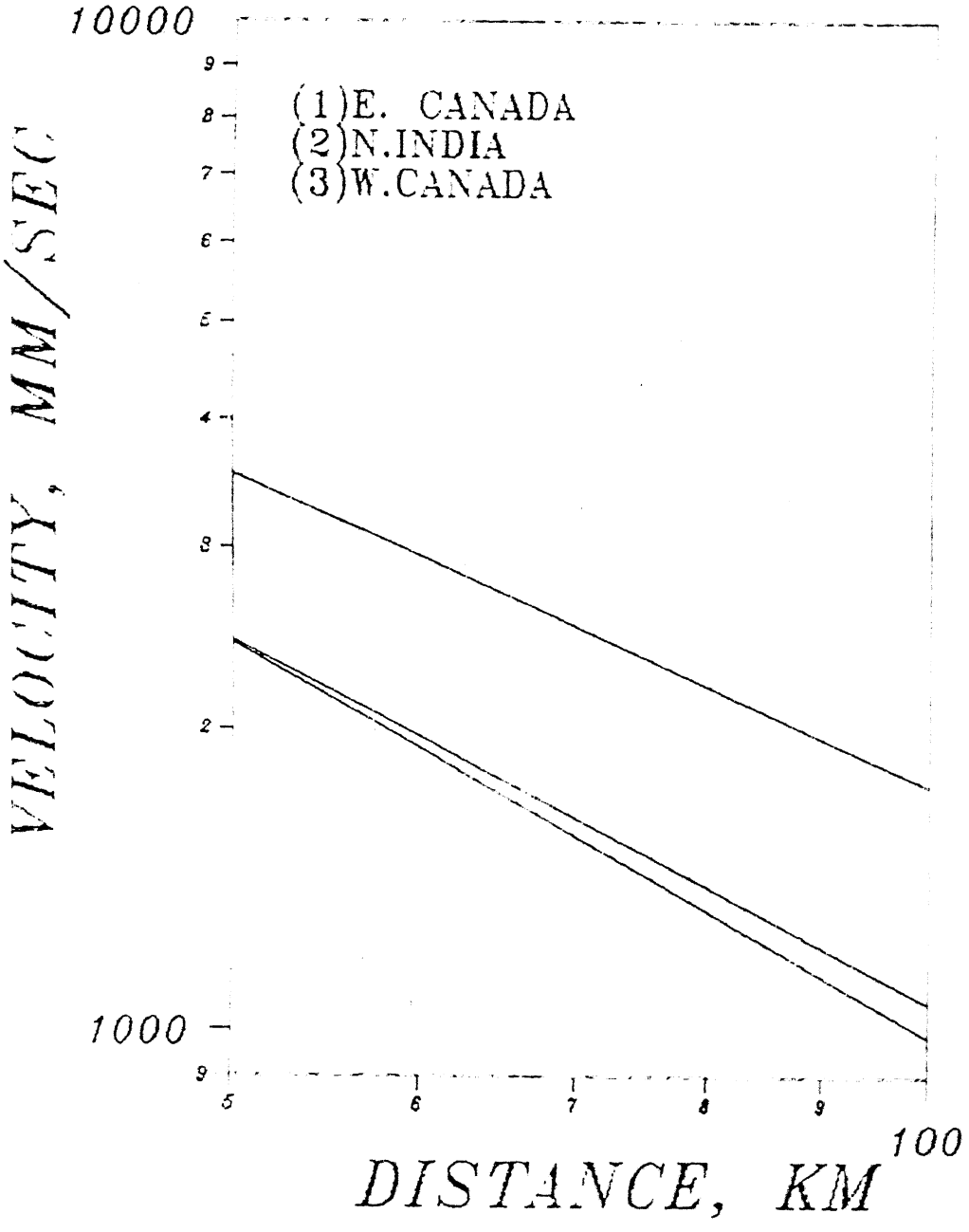

Fig. 4.29 Sample comparison of velocity-distance correlations for various geographical regions using the three variable covariance relations for M = 8.0

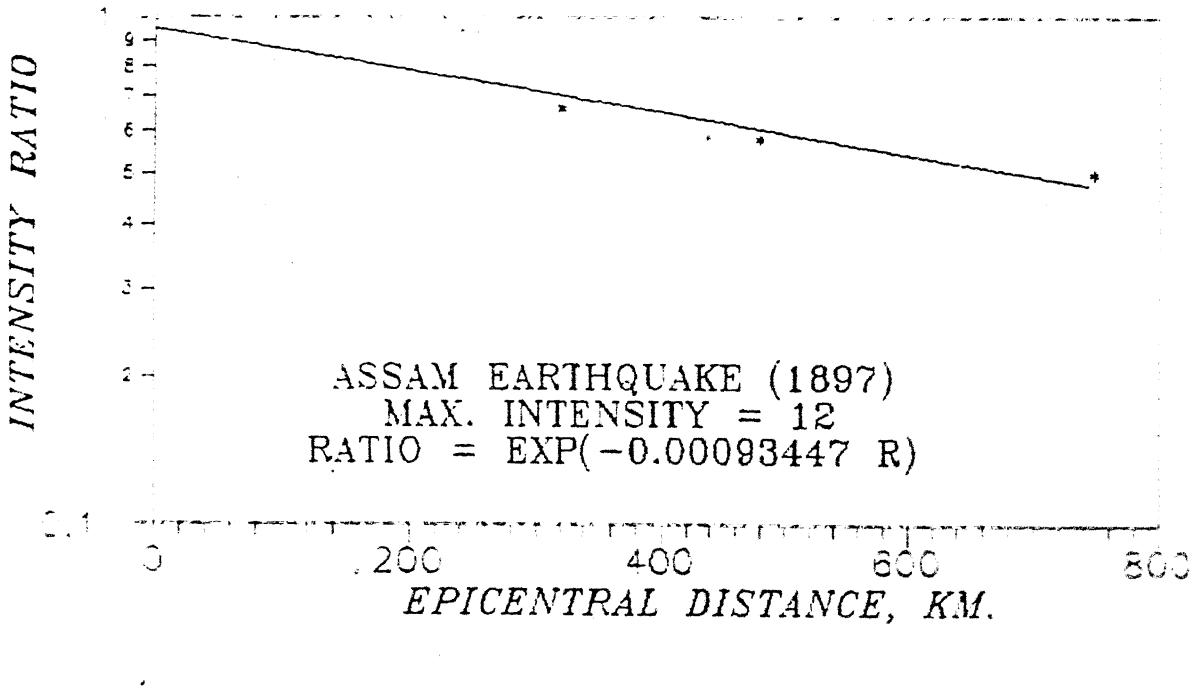

Fig. 4.30 Variation of intensity ratio with epicentral distance for Assam earthquake

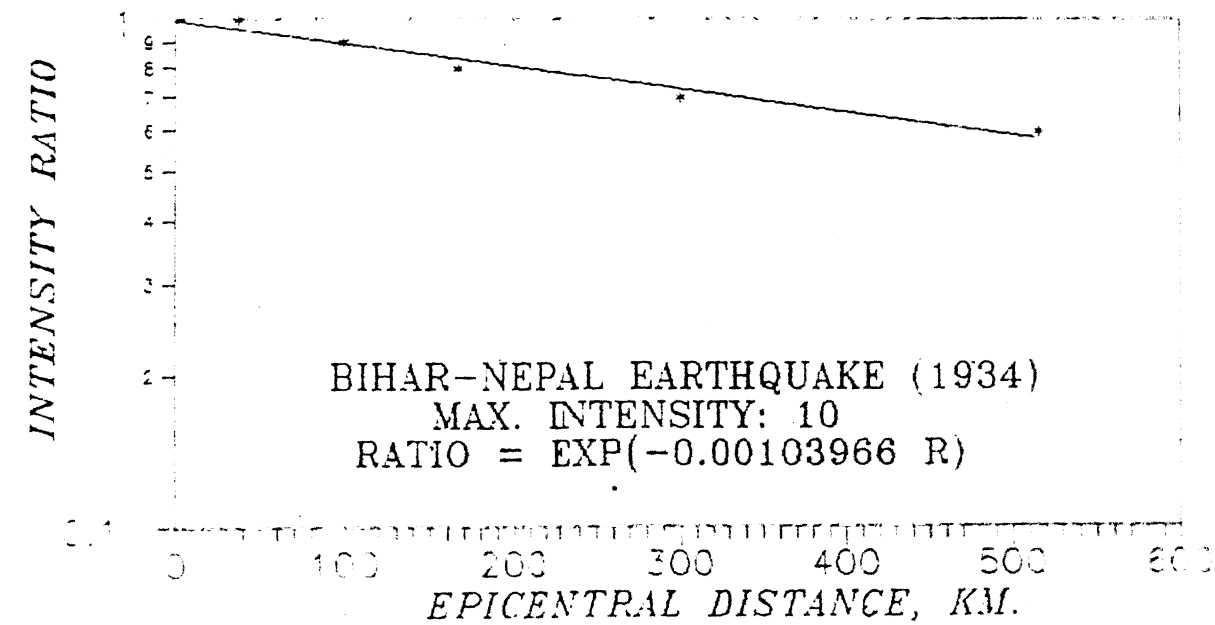

Fig. 4.31 Variation of intensity ratio with epicentral distance for Bihar-Nepal earthquake

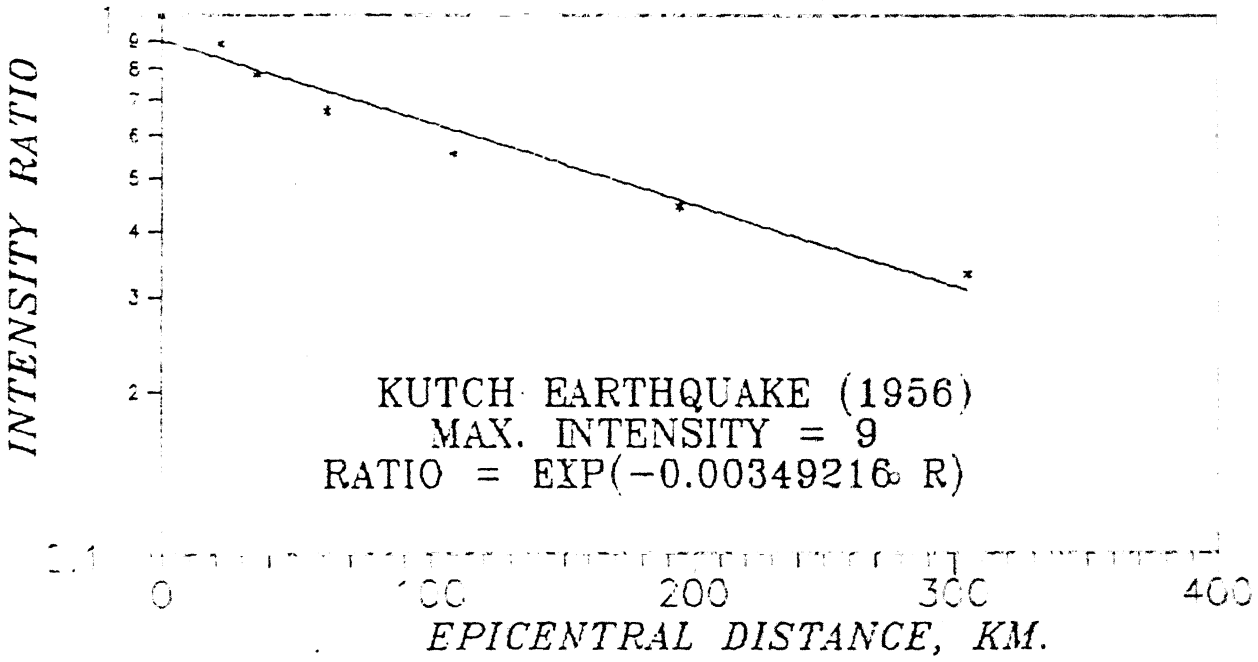

Fig. 4.32 Variation of intensity ratio with epicentral distance for Kutch earthquake

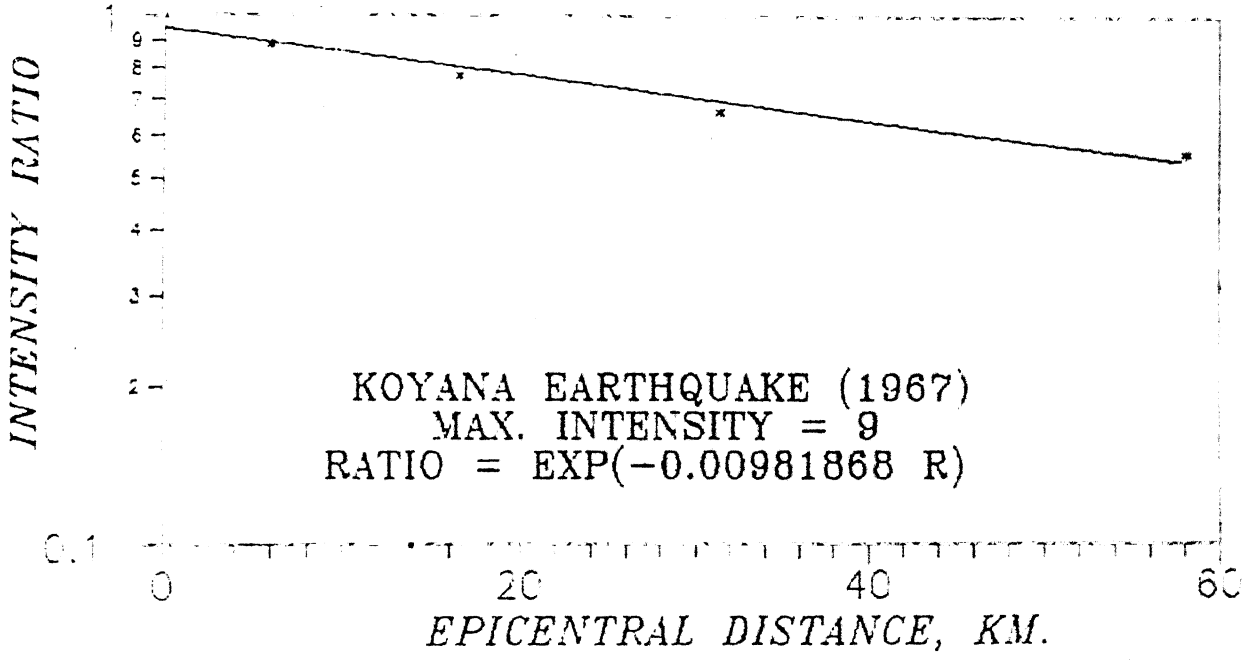

Fig. 4.33 Variation of intensity ratio with epicentral distance for Koyana earthquake

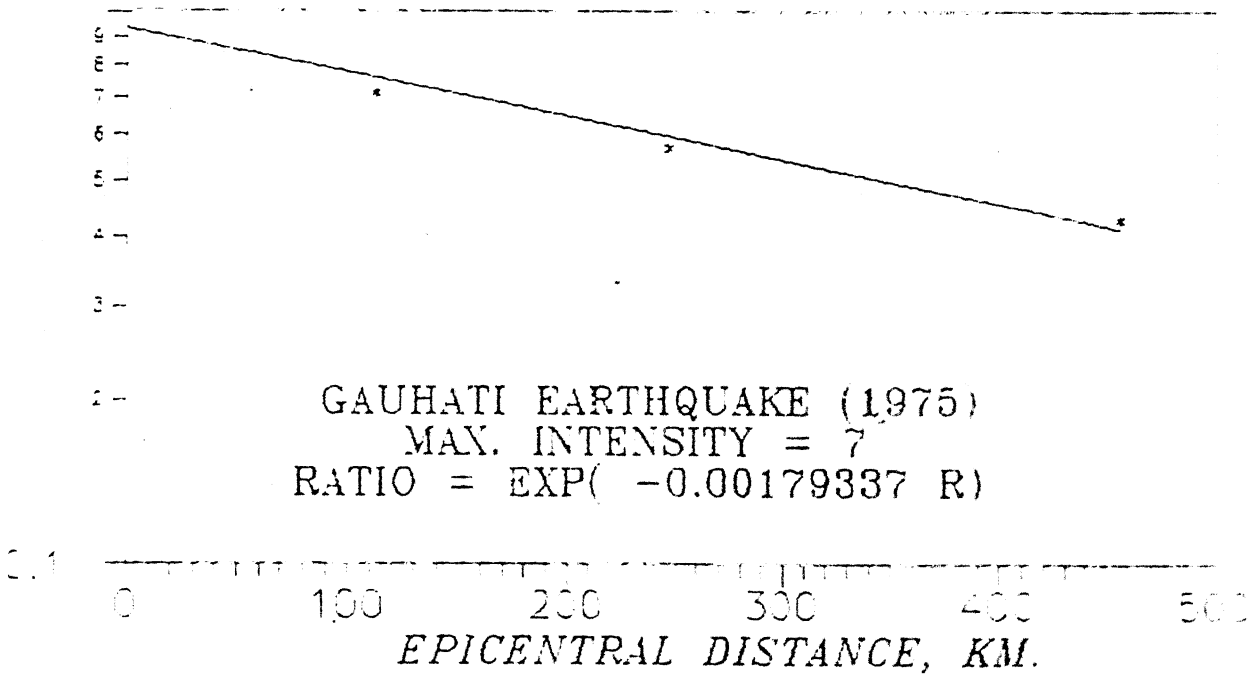

Fig. 4.34 Variation of intensity ratio with epicentral distance for Gauhati earthquake

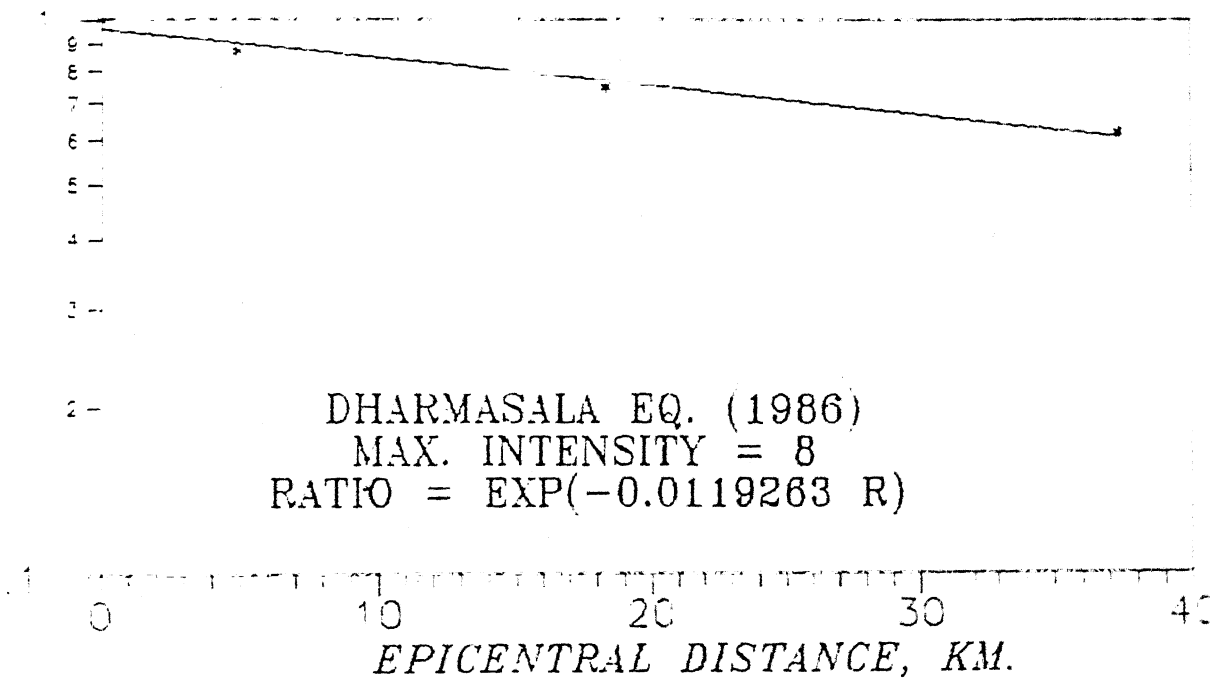

Fig. 4.35 Variation of intensity ratio with epicentral distance for Dharmasala earthquake

epicentral Intensity and k is a coefficient which depends on the slope of the straight line.

Intensity-distance relations obtained for different earthquakes are as follows:

Assam earthquake (Figure 4.30):

$$I/I_0 = e^{-0.000934\Delta} \qquad (4.30)$$

Bihar-Nepal earthquake (Figure 4.31):

$$I/I_0 = e^{-0.0010396\Delta} \qquad (4.31)$$

Kutch earthquake (Figure 4.32):

$$I/I_0 = e^{-0.0034922\Delta} \qquad (4.32)$$

Koyana earthquake (Figure 4.33):

$$I/I_0 = e^{-0.0098187\Delta} \qquad (4.33)$$

Gauhati earthquake (Figure 4.34):

$$I/I_0 = e^{-0.0017933\Delta} \qquad (4.34)$$

Dharmasala earthquake (Figure 4.35):

$$I/I_0 = e^{-0.0119263\Delta} \qquad (4.35)$$

From above relations it is evident that decay rate of intensity is maximum for Dharmasala earthquake (equation 4.35). The attenuation rate of peak horizontal acceleration and peak horizontal velocity have also found to be very high for Dharmasala region (equations 4.11 and 4.20). The higher attenuation rates show the underlying subsurface structures are hard in nature. The decay rate of Intensity with distance from the epicentre for Koyana region (equation 4.33)is also found to be high which is attributed to the harder nature of Deccan trap.

4.8 PEAK HORIZONTAL ACCELERATION-INTENSITY RELATION

Murphy and O'Brien (1977) have proposed a model which shows that the acceleration-intensity correlation is a function of earthquake magnitude and epicentral distance based on world wide data. The relation proposed by Murphy and O'Brien (1977) is

$$\log a = 0.14\ I + 0.24M - 0.68 \log R + \beta \qquad (4.36)$$

where a is the peak horizontal acceleration (cm sec^{-2}), R is the epicentral distance (km) and β is a coefficient which depends upon the data from particular geographical region,

$\beta = 0.60$ for western United States

$\beta = 0.69$ for Japan and

$\beta = 0.88$ for southern Europe. (Murphy and O'Brien 1977).

Using the data given in Table 4.1 and isoseismal maps of various earthquakes, we have proposed a relation similar to the relation given by Murphy and O'Brien (1977) for northern India

$$\log a = 0.14\ I + 0.24M - 0.68 \log R + 0.65 \qquad (4.37)$$

In the above relation, we have used $\beta = 0.65$ for northern India based on very limited earthquake data. To have a more reliable estimate of β, a larger earthquake data base should be used. From Figure 4.36 it is seen that for a geographical region, for example western United States, the relations proposed by various workers show a large deviation. This deviation may be related to difference in the composition and size of the data samples and the techniques adopted by various workers.

Using equations (4.37) and (4.36), we have compared the variation of horizontal acceleration with M.M. intensity, for different geographical regions (Figure 4.37). It has been found

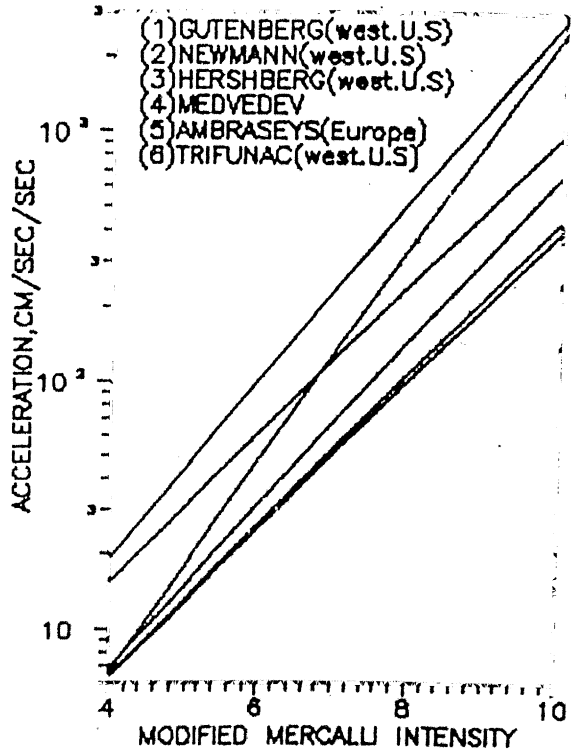

Fig. 4.36 Graphic representation of intensity-acceleration correlations for different geographical regions

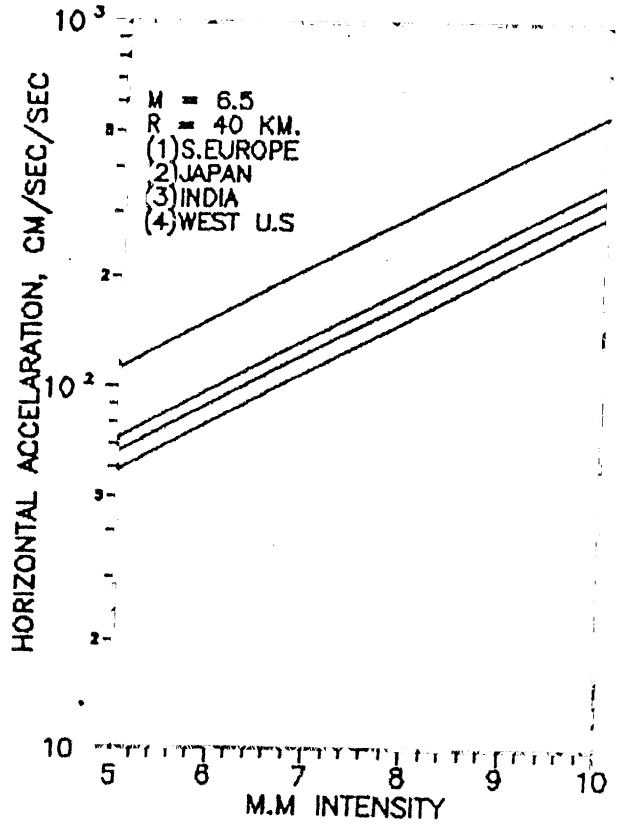

Fig. 4.37 Sample comparison of acceleration -intensity correlations for various geographical regions using the four variable covariance

that the horizontal acceleration is much higher for southern Europe than that of other geographical regions.

CHAPTER V

CONCLUSIONS AND RECOMMENDATIONS FOR FUTURE WORK

5.1 CONCLUSIONS

In the present work, we have developed some empirical relations for various regions of India for estimating peak accelerations and peak velocities during an earthquake. Using these relations, strong ground motion due to an earthquake can be predicted at the site of interest. The knowledge of strong ground motion will be useful in Earthquake Engineering applications, preparation of seismic zoning map and in the correlation of subsurface geological structure.

The attenuation relations have been proposed based on the observed seismological data of past earthquakes. These relations correspond to earthquakes occurring in different regions. Using these relations, peak horizontal accelerations and peak horizontal velocities have been calculated and their variations are graphically illustrated with the distance from the hypocentre/epicentre of an earthquake . We have found that the strong ground motion of different earthquake show characteristic behavior. The behavior of strong motion is dependent on the earthquake parameters i.e., magnitude and intensity, and also significantly dependent on the geology of the epicentral regions. In our present study, we have not taken geological consideration due to lack of geological information and it is assumed that the recorded strong motion data would reflect the nature of the subsurface. Based on the attenuation relations of different regions of India, we have given an empirical relation for northern India (equation 4.37). This relation is based on limited

earthquake data observed during major earthquakes in the northern region of India. Most of the constants used in the equation (4.37) are adopted based on the world wide data. For an accurate and reliable estimate of ground motion in the northern India, the constants used in different attenuation relations should be estimated based on detailed observations during earthquakes and on large strong motion database.

We have compared the attenuation relations developed for northern India with those of Canada and other geographical regions. We have found that, for higher magnitudes, peak horizontal acceleration values are higher in case of northern India to those of Canada. For lower magnitudes, peak horizontal acceleration values are found higher for Canada to those of northern India. From this observation, it has been concluded that higher magnitude earthquakes in India produce comparatively higher accelerations. Peak horizontal velocities are observed to be similar for both northern India and western Canada. It has also been found that ground motion values are lower for northern India than those of southern Europe.

Finally, we have derived intensity attenuation relations based on the idealised circular isoseismal contours. These equations represents decay rate of intensity with distance from the epicentre. Intensity attenuation relations can be used to estimate the level of possible destruction that would be caused by future earthquakes. Thus, the intensity-distance relations have wide applicability in the prediction of the level of damage in a region due to a earthquake.

5.2 RECOMMENDATIONS FOR FURTHER WORK

The present work is based on the limited earthquake and strong motion data. For a reliable and accurate estimate of strong ground motion at the site of interest, we bring out following points which should be kept in mind for future studies.

(1) The reliability of the attenuation relations derived in the form of equation (4.1) depends on the size of the database used for the estimation of the attenuations b_1, b_2 and b_3 of equation (4.1). In the present work, we have used strong motion data from five different earthquakes. More reliable estimation of the attenuation constants b_1, b_2 and b_3 can be made using the strong motion data obtained from the recent earthquakes.

(2) In the present work, strong motion equations developed do not depend on the nature of the site geology. One can study the effect of site geology on the ground motion and can develop empirical relations for different regions.

(3) In developing relationships for estimating ground motion, we have not considered the effect of type of fault. The effect of type of fault on different measures of strong motion should be studied by adopting suitable attenuation model.

(4) Detailed earthquake observation has been made along 2500 km long Himalayan belt for the further refinement of attenuation relations developed in the present work.

REFERENCES

Ambraseys, N. N. (1972), Behaviour of foundation materials during strong earthquakes, Proc. European Sympo. Earthquake Engr., 4th, London.

Ambraseys, N. N. (1972a), The correlation of intensity with ground motions, Proc. European Conf. Earthquake Engr., 4th, Trieste, pp. 1-12.

Ambraseys, N. N. (1972b), Dynamics and response of foundation materials in empirical regions of strong earthquakes, Proc. World Conf. Earthquake Engr., 5th, Rome.

Campbell, K.W. (1989), The dependence of peak horizontal acceleration on magnitude, destance, and site effects for small magnitude earthquakes in California and Eastern North America. Bull. Seism. Soc. Am., Vol. 79, pp. 1311-1346.

Choudhury, S.K. (1975), Gravity and crustal thickness in the Indo-Gangetic plains and Himalayan region, India. Geophys. J. R. Astron. Soc., Vol. 40, pp. 441-452.

Dewey, J.F. and Bird, J.M. (1970), Mountain belts and the new global tectonics. J. Geophys. Res., Vol. 75, pp. 2625-2647.

Espinosa, A.F. (1977), Particle-velocity attenuation relations: San Fernando earthquake of February 9, 1971. Bull. Seism. Soc. Am., Vol. 67, pp. 1195-1214.

Esteva, L. (1970), Seismic risk and seismic design decisions. Seismic design for nuclear power plants, R. J. Hansen, Editor, M. I. T. press, pp. 142-182.

Fitch, T.J. (1970), Earthquake mechanism in the Himalayan, Burmese and Andaman regions and continental tectonics of central Asia. J. Geophys. Res., Vol. 75, pp. 2699-2709.

Gubin, I. (1969), Earthquakes and seismic zoning of Indian peninsula. CWPC Press, New Delhi.

Guha, I.E. (1962), Seismic Regionalisation of India. Proc of 2 nd Symposium on Earthquake Engineering, University of Roorkee, U.P., India.

Gupta, H.K. Narain, H. Rastogi B.K. and Mohan I. (1969), A study of the Koyana earthquake of December 10, 1967. Bull. Seism. Soc. Am., Vol. 59, pp. 1149-1162.

Gupta, H.K. Narain, H. and Mohan I. (1970), The Godavari earthquake sequence of April 13, 1969. Bull. Seism. Soc. Am., Vol. 60, pp. 601-615.

Gupta, H.K. Rastogi, B.K. and Narain, H. (1971), The Koyana earthquake of December 10, 1967: A multiple seismic event. Bull. Seism. Soc. Am., Vol. 61, pp. 161-176.

Gupta, K.H. (1980), Recent long period surface wave dispersion investigations in the Himalaya and neighbouring regions. Indian

Gutenberg, B. and Richter, C.F. (1956), Earthquake magnitude, Intensity, energy and acceleration. Bull. Seism. Soc. Am., Vol. 46, pp. 105-146.

Hasegawa, H.S. Basham, P.W. and Berry, M.J. (1980), Attenuation relations for strong seismic ground motion in Canada. Bull. Seism. Soc. Am., Vol. 71, pp. 1943-1962.

Holmes, A. (1966), Principles of physical geology. Ihomas nelson, London, Edinburgh, pp. 1288.

Joyner, W.B. and Boore, D.M. (1991), Strong earthquake ground motion and engineering design. Geotechnical News, Vol 9, pp. 21-26.

Kaila, K.L. and Sarkar, D. (1978), Atlas of isoseismal maps major earthquakes in India. Geophysical Reasearch Bulletin. Vol. 16. No. 4, pp. 233-265.

Kanai, K. (1961), An empirical formula for the spectrum of strong earthquake motions. Bull Earthquake Res. Inst., Tokyo University, Vol. 39, pp. 85-95.

Murphy, J.R. and Lahoud, J.A. (1969), Analysis of seismic peak amplitudes from underground nuclear explosions. Bull Seism Soc. Am., Vol. 59, pp. 2325-2342.

Murphy, J.R. and O'Brien, L.J. (1977), The correlation of peak ground acceleration amplitude with seismic and other physical parameters. Bull. Seis. Soc. Am., Vol. 67, pp. 877-915.

Newmark, N.M. and Rosenblueth, E. (1971), Fundamentals of Earthquake Engineering. Printice Hall, Englewood Cliffs, New Jersey. pp. 219.

Orphal, D.L. and Lahoud, J.A. (1974), Pridiction of peak ground motion from earthquakes. Bull. Seism. Soc. Am., Vol. 64, pp. 1563-1574.

Richter, C.F. (1958), Elementary Seismology. Freeman & Co., San Francisco, pp. 397.

Sabetta, F. and Pugliese, A. (1987), Attenuation of peak horizontal acceleration and velocity from Italian strong-motion records, Bull. Seism. Soc. Am., Vol. 72

Schnbel, P.B. Seed, H.B. (1973), Accelerations in rock for earthquakes in the western United States. Bull. Seism. Am., Vol. 63, pp. 501-516.

Singh, D.D. and Gupta, H.K. (1980), Source dynamics of two great earthquakes of Indian subcontinent: The Bihar-Nepal earthquake of January 15, 1934 and the Quetta earthquake of may 30, 1935. Bull. Seism. Soc. Am., Vol. 70, pp. 757-773.

Taheri, J.S. and Anderson, J.G. (1988), The 1978 Tabas, Iran, Earthquake: An interpretation of the strong motion records. Bull.

Seis. Soc. Am., Vol. 78, pp. 142-171.

Tandon, A.N. (1953), The very great earthquake of August 15, 1950. Central Board of Geophysics- A compilation of papers on Assam earthquakes of 1950, 1963. pp. 80-89.

Trifunac, M.D. and Brady, A.G. (1975), On the correlation of seismic intensity scales with the peaks of recorded strong ground motion. Bull. Seism. Soc. Am., Vol. 64, pp. 1563-1574.

Valdiya, K.S. (1964), The unfossiliferous formations of the lesser Himalaya and their correlation. Proc. 22 nd Int. Gol. Congr., 11, pp. 15-36.

Valdiya, K.S. (1976), Himalayan transverse faults and folds and their parllelism with subsurface structures of north Indian plains. Tectonophysics, Vol. 32, pp. 353-386.

A 112568

CE-1991-M-PRA-ATT